DEVELOPMENT OF A MICRO-WELL-BASED MICROFLUIDIC 3D CELL
CULTURE FOR CYTOTOXICITY ASSAY

A THESIS SUBMITTED TO
THE GRADUATE SCHOOL OF NATURAL AND APPLIED SCIENCES
OF
MIDDLE EAST TECHNICAL UNIVERSITY

BY

SARAH FARAHANI

IN PARTIAL FULFILLMENT OF THE REQUIREMENTS
FOR
THE DEGREE OF MASTER OF SCIENCE
IN
MICRO AND NANOTECHNOLOGY

JANUARY 2023

Approval of the thesis:

DEVELOPMENT OF A MICRO-WELL-BASED MICROFLUIDIC 3D CELL CULTURE FOR CYTOTOXICITY ASSAY

submitted by **SARAH FARAHANI** in partial fulfillment of the requirements for the degree of **Master of Science** in **Micro and Nanotechnology, Middle East Technical University** by,

Prof. Dr. Halil Kalıpçılar
Dean, Graduate School of **Natural and Applied Sciences**   _____

Prof. Dr. Deniz Üner
Head of the Department, **Micro and Nanotechnology**   _____

Assoc. Prof. Dr. Ender Yıldırım
Supervisor, **Micro and Nanotechnology Dept., METU**   _____

Assist. Prof. Dr. Altuğ Özçelikkale
Co-Supervisor, **Mechanical Engineering Dept., METU**   _____

Examining Committee Members:

Prof. Dr. Haluk Külah
Electrical and Electronics Eng. Dept., METU   _____

Assoc. Prof. Dr. Ender Yıldırım
Mechanical Engineering Dept., METU   _____

Assist. Prof. Dr. Altuğ Özçelikkale
Mechanical Engineering Dept., METU   _____

Assoc. Prof. Dr. Hüseyin Cumhur Tekin
Bioengineering Dept., Izmir Institute of Technology   _____

Assist. Prof. Dr. Ahmet Acar
Dept. of Biological Sciences, METU   _____

Date: 26.01.2023

I hereby declare that all information in this document has been obtained and presented in accordance with academic rules and ethical conduct. I also declare that, as required by these rules and conduct, I have fully cited and referenced all material and results that are not original to this work.

Name Last name : Sarah Farahani

Signature :

ABSTRACT

DEVELOPMENT OF A MICRO-WELL-BASED MICROFLUIDIC 3D CELL CULTURE FOR CYTOTOXICITY ASSAYS

Farahani, Sarah
Master of Science, Micro and Nanotechnology
Supervisor: Assoc. Prof. Dr. Ender Yıldırım
Co-Supervisor: Assist. Prof. Dr. Altuğ Özçelikkale

January 2023, 80 pages

This thesis presents a micro-well-based microfluidic platform's design, optimization, simulation, and fabrication for 3D cell culture. This work aims to create a system suitable for monitoring cytotoxicity assays on isolated chambers. In this context, microfluidic systems are promising for screening cell response to drugs. Here, a PMMA-based and pipette-operated microfluidic device for cytotoxicity assay is presented. The platform is incorporated into a channel and micro-chamber attached to the sidewall of the channel. The goal is to encapsulate two types of MCF-7 cell-laden 3D collagen matrix namely as Red Fluorescent Protein (RFP)-MCF-7 cells and Wild-Type MCF-7 cells inside each well to form a 3D cell culture that can monitor the culture's response to different drug stimuli.

This design is based on a level-set capillary flow of two multiphase flows, and the goal is to isolate the liquid inside a chamber. Based on the results obtained from Finite Element Analysis (FEA) simulations, a circle-shaped chamber, with a 2 mm diameter, placed at the intersection of the width of the rectangle-shaped channel, demonstrates the highest volume ratio of liquid confinement in the chamber.

In the fabrication process, a micro-milling device is utilized to mill the structure on the PMMA substrate. The processed PMMA is sealed by surface-treatment-assisted thermo-compressive bonding of a blank PMMA sheet.

The fabricated device is then tested by (RFP)-MCF-7 cell-laden 3D collagen matrix and Wild-Type MCF-7 cell-laden 3D collagen matrix. The cell suspension is at first pipetted through the inlet of the channel. As the mixture flows through the channel, it fills the chamber. Vacuuming the channel enables cell-laden collagen confinement in the chamber as well as chamber isolation.

According to the observation of RFP-MCF-7 cell-laden 3D collagen matrix cultured in micro-wells, during a total of 48 hours of monitoring, the results show the success of cell growth in the wells in the first 24 hours of the experiment. The next 24 hours of the experiment were associated with the effect the of doxorubicin anticancer drug with 1µM and 10 µM concentrations on the cells, a dye-based live-dead assay was used to observe the viability of the cells during the experiment. Thus, Hoechst 33342 (blue fluorescence) and Propidium iodide (red fluorescence) were added to the suspension for the observation of live and dead cells, respectively. The corrected total cell fluorescence (CTCF) area was calculated for all control, 1µM treatment, and 10 µM treatment groups. Analyzing both fluorescent and Bright Field (BF) images of quantitative data regarding the effect of the treatment showed a decrease in the level of blue fluorescence and an increase in the intensity of dead cells as a red signal after 24 hours.

Here, theoretical concepts, simulations of Finite Element Analysis (FEA), and the results of tests are discussed separately.

Keywords: 3D cell culture, microfluidics, drug research, cytotoxicity assays

ÖZ

SİTOTOKSİSİTE TESTI İÇİN MİKRO KUYU TABANLI MIKRO AKIŞKAN 3 BUYUTLU HÜCRE KÜLTÜRÜNÜN GELİŞTİRİLMESİ

Farahani, Sarah
Yüksek Lisans, Mikro ve Nanoteknoloji
Tez Yöneticisi: Doç. Dr. Ender Yıldırım
Ortak Tez Yöneticisi: Dr. Öğr. Üyesi. Altuğ Özçelikkale

Ocak 2023, 80 sayfa

Bu tez, 3D hücre kültürü için mikro-kuyu tabanlı bir mikroakışkan platformun tasarımı, optimizasyonu, simülasyonu ve imalatını sunar. Bu çalışma, izole edilmiş odalarda sitotoksisite analizlerinin izlenmesi için uygun bir sistem oluşturmayı amaçlamaktadır. Bu bağlamda, mikroakışkan sistemler ilaçlara hücre yanıtını taramak için umut vericidir. Burada, sitotoksisite deneyi için PMMA tabanlı ve pipetle çalışan bir mikroakışkan cihaz sunulmaktadır. Platform bir kanala dahil edilmiştir ve kanalın yan duvarına bağlı mikro-ocak. Amaç, iki tip MCF-7 hücre yüklü 3D kollajen matrisini, yani kırmızı floresan protein (RFP) -MCF-7 hücreleri ve vahşi tip MCF-7 hücrelerini, her oyuk içinde izleyebilen bir 3D hücre kültürü oluşturmak için kapsüllemektir. Kültürün farklı ilaç uyaranlarına yanıtı.

Bu tasarım, iki çok fazlı akışın seviye ayarlı kılcal akışına dayanmaktadır ve amaç, bir odadaki sıvıyı izole etmektir. Sonlu eleman analizi (FEA) simülasyonlarından elde edilen sonuçlara dayanarak, 2 mm çapında, dikdörtgen şekilli kanalın genişliğinin kesişimine yerleştirilmiş daire şeklindeki bir bölme, odadaki en yüksek hacim oranını gösterir.

İmalat işleminde, yapıyı PMMA substratı üzerindeki değirmeni yapmak için bir mikro değirmencilik cihazı kullanılır. İşlenen PMMA, boş bir PMMA tabakasının yüzey tedavi destekli termo-baskıcı bağı ile kapatılır.

Fabrikasyon cihaz daha sonra (RFP) -MCF-7 hücreli 3D kollajen matrisi ve vahşi tip MCF-7 hücre yüklü 3D kollajen matrisi ile test edilir. Hücre sspention ilk önce kanalın girişinden pipetlenir. Karışım kanaldan akarken, odayı doldurur. Kanalın vakumlanması, odada hücre yüklü kollajen sınırlarını ve oda izolasyonunu sağlar.

Mikro-kuyularda kültürlenen RFP-MCF-7 hücre yüklü 3D kollajen matrisinin gözlemine göre, 48 saatlik bir izleme sırasında, sonuçlar xeperiment'in ilk 24 saatinde kuyularda hücre büyümesinin başarılı olduğunu göstermektedir. Denemenin sonraki 24 saati, hücreler üzerinde 1µm ve 10 um konsantrasyonlara sahip doksorubisin antikanser ilacının etkisi ile ilişkili olduğundan, deney sırasında hücrelerin canlılığını gözlemlemek için boya bazlı bir canlı ölü test kullanıldı. Böylece, canlı ve ölü hücrelerin gözlemlenmesi için süspansiyona Hoechst 33342 (mavi floresan) ve propidyum iyodür (kırmızı floresan) ilave edildi. Düzeltilmiş toplam hücre floresanı (CTCF) alanı, tüm kontrol, 1µm tedavi ve 10 uM tedavi grupları için hesaplandı. Tedavinin etkisine ilişkin hem floresan hem de parlak alan (BF) görüntülerinin analiz edilmesi, mavi floresan seviyesinde azalma ve 24 saat sonra kırmızı tekli olarak ölü hücrelerin yoğunluğunda artış olduğunu gösterdi.

Burada teorik kavramlar, sonlu element analizi (FEA) simülasyonları ve testlerin sonuçları ayrı ayrı tartışılmaktadır.

Anahtar Kelimeler: 3D hücre kültürü, mikroakışkan, ilaç araştırması, sitotoksisite deneyleri
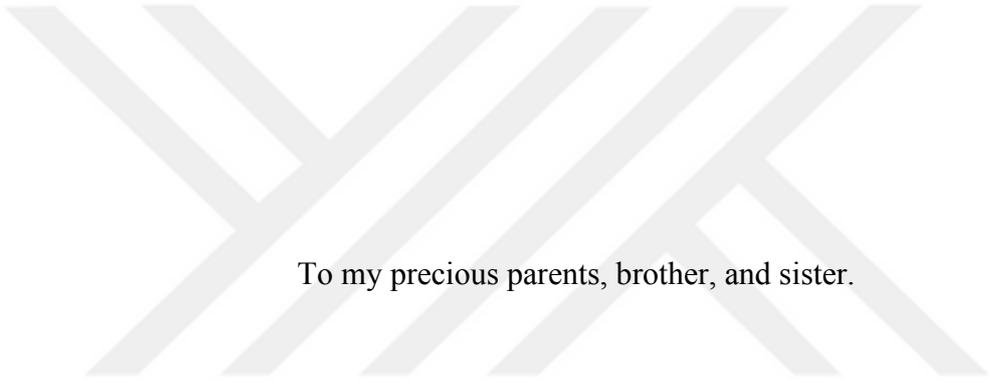
To my precious parents, brother, and sister.

ACKNOWLEDGMENTS

I would like to express my sincere gratitude to my supervisor, Prof. Dr. Ender Yıldırım, for his invaluable support and guidance throughout my research. His mentorship not only contributed to my academic success but also provided me with valuable insights into real-life applications. Working with Professor Yıldırım has been a truly transformative experience, and his encouragement has motivated me to strive for a greater impact in both academia and society.

I am also deeply grateful to my co-advisor, Prof. Altuğ Özçelikkale, for his continuous support, guidance, and valuable insights throughout my research journey. I am thankful for the opportunity to work with him and for his role in shaping my research direction.

I would like to extend my thanks to the members of the micro-manufacturing lab, Ayşen Gümüştaş, Erdem Bayraktar, Görkem Başabaşı, Mert Kerem Ülkü, Ufuk Dirmencioglu, Mert Nakisli, and Miray Sanem Sarı for their time, support, and friendship. Their help has been instrumental in the completion of this thesis.

I also had the privilege to collaborate with Barış Dedekargınoğlu, Hakan Berk Aydın, and Milad Fathi from the Engineered Biomicrosystems Laboratory (EBL) research group. I am deeply grateful for their support, expertise, and collaboration in the 3D cell culture aspect of the research.

I would like to also thank my friends Nayere Fallah Bagheri and Shima Rezaee for their support and encouragement throughout my academic journey. Their friendship has been a constant source of motivation and inspiration. I am grateful for their presence in my life.

I owe an immeasurable debt of gratitude to my parents, Sedigheh and Hamidreza Farahani, and my siblings, Hamed and Sahar, for their unwavering support and

encouragement throughout my academic journey. Their constant inspiration and encouragement have been a driving force behind my success.

TABLE OF CONTENTS

LIST OF TABLES

LIST OF FIGURES

FIGURES

xviii

CHAPTER 1

INTRODUCTION

Living cell functionality, in complex organ/tissue environments, requires an intuition that helps to comprehend the physiological and pathophysiological subordinate in the human body [1, 2]. Several regulations are required for cell function, survival, and growth in the human body, which are demonstrated in the chemical gradients and mechanical forces such as compression and sheer stress by cells as specific dynamic variations [3]. The use of conventional two-dimensional (2D) cell cultures for molecular mechanism and cellular function examination back over a century. Nevertheless, neither the data related to the complication of the living system nor the differentiation and tissue specification of various and plenty of cell types can be provided by these cultures [4]. In many research works, 2D cultures are still the most favorable approach. However, to represent the way that cells grow and continue their functions or the way that diseases and damages in nature affect them, there is a need for a three-dimensional (3D) microenvironment, and results from a flat surface in 2D models cannot be an accurate demonstration because cell's ability for recapitulation of the proper levels of in vivo cellular responses is considerably confined as shown in Fig. 1-1 [5]. The lack of a physiological matrix-like microenvironment prevents differentiation and normal growth to occur, even when the medium prepares diverse necessary constituents and other growth factors [6, 7]. As a consequence, a lot of research and effort has been done to prove that the efficiency has shifted from 2D models to 3D models which aim to mimic the cell's physiologically relevant environment and thus provide a better efficiency has shifted from 2D models to 3D models which aim to mimic the cell's physiologically relevant environment and thus provide a better microenvironment for them which is more predictive than 2D

1

models [8, 9]. In this regard, the way that modern biology is performed can be significantly altered since microfluidic systems offer advantages such as smaller volumes of reagents, executing parallel operations, and reducing the reaction times compared to conventional assays. Moreover, transferring a complete laboratory into a single chip (i.e., Lab-on-chip) is another promise offered by these systems. Besides the classic advantages of miniaturization, the most important potential lies in micro-scale physics. As it has been proved that there are techniques and experiments which are not able to be performed on the macro scale if microscale phenomena can be comprehended in microfluidic systems, eventually the probability of making functionality and new empirical executions into action comes true.
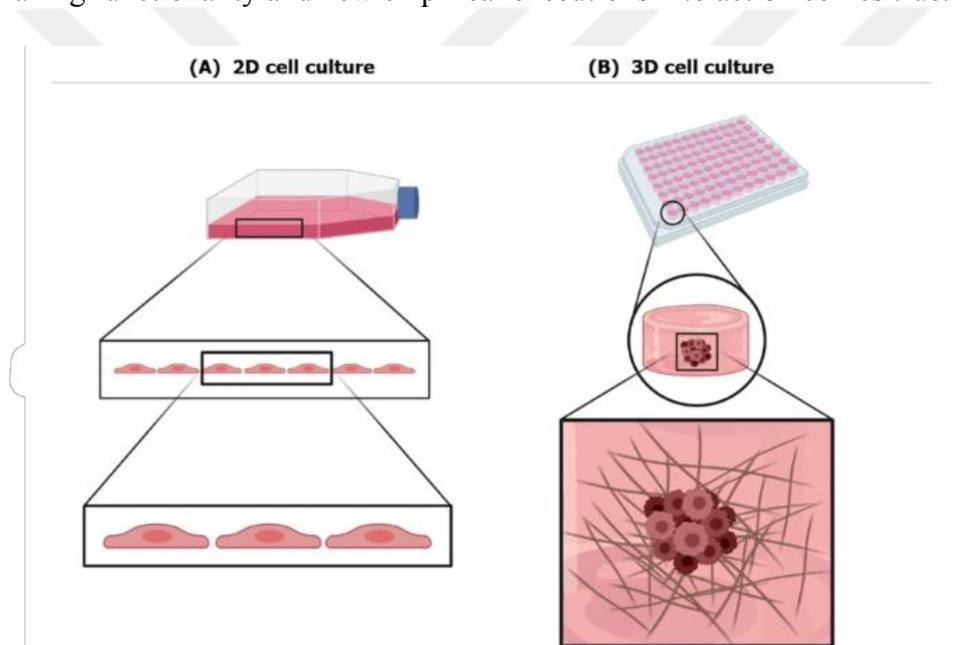
Figure 1-1. A comparison between 2D and 3D cell culture. (a) The behavior of cells cultured in a conventional 2D platform. Cell morphology cannot be represented in a 2D platform since cells are cultured on a flat substrate. (b) The behavior of cells cultured in a 3D platform. The culture method in 3D resembles a microenvironment alike to that in vivo in which cells can represent a more similar morphology and shape of cells in the body [10].

To have a better biomimetic tissue model, there is a need to transfer from 2D cell culture to 3D techniques. By being able to engage spatial co-cultures, signal control,

and perfusion flow microfluidic systems have become considerably valuable as a tool that will make the development of relevancy of physiological aspects in 3D culture further and so, fluids in micro-channels are characterized with spatial control. There has been much research conducted to develop microfluidic-based 3D culture platforms to allow more precise methods for cell-based assays. Spheroids which technically are various cell lines living together in a 3D format are one of the most promising methods in this context, and research inquiries have claimed to form spheroids from different cell lines in microfluidic devices [11, 12, 13].

1.1   Motivation

Researchers have been striving to devise novel techniques for cell culture to enhance the relevance of in vitro experiments and mimic cellular behavior in living tissues. The primary objective of these methods is to replicate the microenvironment that cells experience in the body. In this regard, microfluidic-based 3D cell culture platforms offer promising opportunities for analysis due to their ability to integrate biological complexity with practical production procedures. Compared to conventional two-dimensional cell culture formats, 3D cell cultures allow for better biological function as cells can interact with neighboring cells in a more physiologically relevant environment.

However, isolating cell-laden gels in a microfluidic 3D cell culture platform can be challenging. This thesis proposes a well-array composed of cylindrical micro-chambers at one side of a microchannel as an alternative means for 3D cell culturing. Cell-laden hydrogels are aimed to be isolated in these chambers where the cells can be cultured, or cytotoxicity assays can be carried out. Since the cells and thus the culture environment is confined in the chambers, it is claimed that the proposed method solves the problems of accessing and isolation problems currently observed in the existing microfluidic platforms.

1.2   The Objective of the Thesis

This work proposes a microfluidics micro-well array to isolate cell-laden gel and confine liquid inside them for cytotoxicity assays. The objectives of the thesis are as follows:

- Design of a microfluidic chip that can be pipette operated.
- To design a chip made of thermoplastic substrates to enable scalable manufacturing.
- To model the flow using Finite Element Analysis (FEA) method.
- To optimize the wells using the (FEA) model.
- To demonstrate the chip operation using MCF-7 cells.
- To propose a method for scalable manufacturing of the microfluidic chip

Hence, for these purposes, we propose a pipette-operated device consisting of in-line micro-wells connected to a microchannel with a specific angle between the channel sidewall and wells.

The working principles of the chip can be summarized as follows:

1. In the first step, we introduce cell-containing hydrogel through an inlet (Fig. 1-2. a-b).
2. After the whole channel and chambers are filled with cell-laden hydrogel, we flush away the excess hydrogel in the channel by introducing the oil flowing in the channel through the inlet port (Fig. 1-2. c). Since they are immiscible, the hydrogel in the channel gets out of the outlet, leaving the hydrogel in the chamber isolated (Fig. 1-2. d). Then, the chambers are left for a certain period for gelation.
3. For feeding the cells, the oil is flushed away using a medium flowing in the channel injected through the inlet.

Fig. 1-2 shows the working principles of the microfluidic chip.
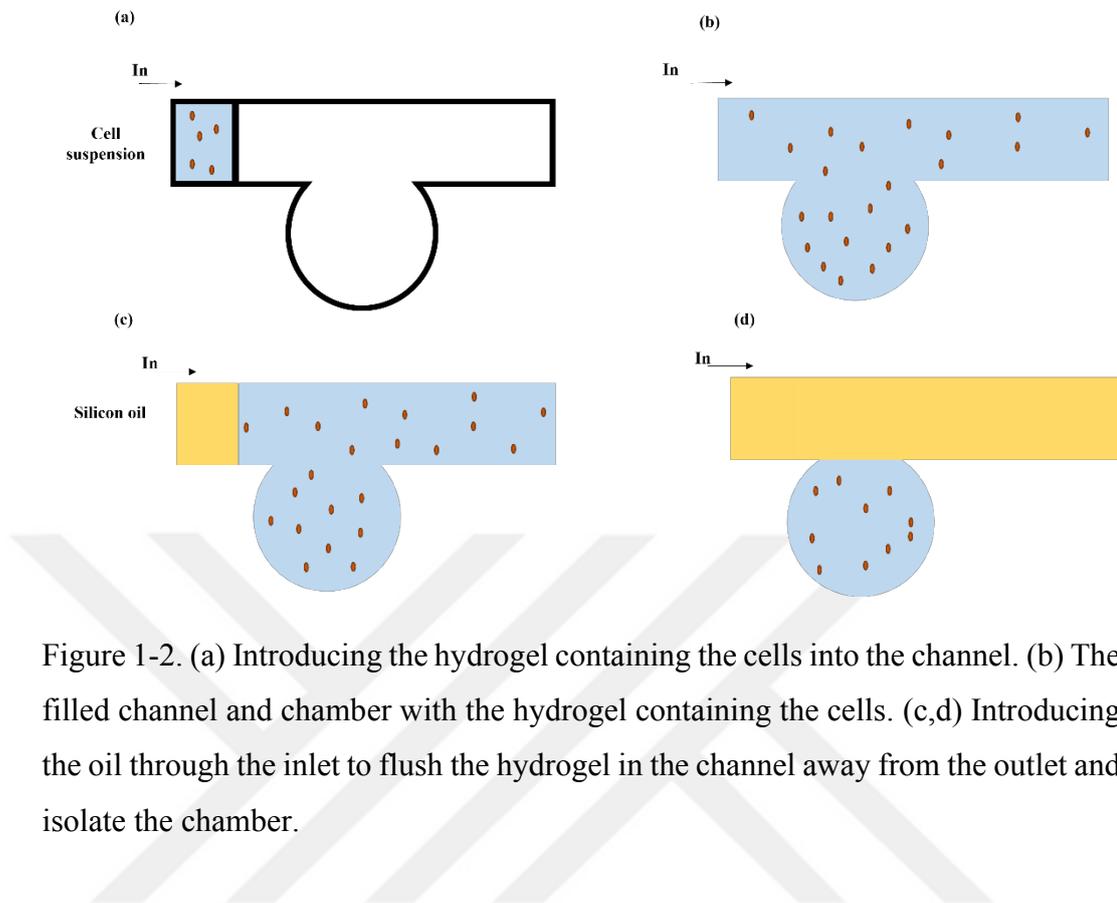
Figure 1-2. (a) Introducing the hydrogel containing the cells into the channel. (b) The filled channel and chamber with the hydrogel containing the cells. (c,d) Introducing the oil through the inlet to flush the hydrogel in the channel away from the outlet and isolate the chamber.

CHAPTER 2

LITERATURE REVIEW

Cell culture started when scientists could harvest cells taken from animal tissue and culture them or keep them in a specific media for further steps [14, 15]. The comprehension of necessary considerations regarding cell health and the longevity of their existence increased as the interest in various cell lines was raised [16]. This was a spark of growth in parts and then fully synthetic media for cell culture from the 1900s up to now [17]. Based on the American Type Culture Collection report, more than 3600 cell lines are available which have been organized from over 150 diverse species that are a result of growth in synthetic culture [18]. The usage of these vastly accessible cell lines has enabled researchers to enlarge our appreciation of the process of formatting and the functionality of tissues in the body, which results in major enhancements and advances in medicine and health [16]. As we can consider cell culture as an alternative method that can substitute organ culture and in vivo testing, it is also a bridge of connection in several ongoing studies affecting medical research including biochemistry, pharmacokinetics, biology, tissue engineering, and drug discovery [19]. Cell culture methods provide a platform that is accessible, quite reproducible, and dependable mode of research [20] as well as providing better clarification of a process before further preclinical and human studies get started [21].

2.1   A Review of 3D Cell Culture

To maintain, retain, and analyze the adherent cell lines, 2D or monolayer cell culture has been used over the past century, and it has been the most popular method [22,

23]. In this method, the maintenance of cells is conducted on a flat substrate such as Petri-dishes or micro-titer plates (Fig. 2-1). The surface functionalization can be readily done using proteins or other surface components which can help to modify the adhesion of cell health [24, 25, 26]. Retaining cells in these flasks are low cost, and since there are developed protocols that are robust and simple the tendency of contamination is reduced. Monitoring cell viability and morphology can be easily performed by directly imaging through these dishes. Moreover, analyzing the effect of a variety of conditions and simulations applied to the sample due to adding new reagents is easy to achieve [22, 8]
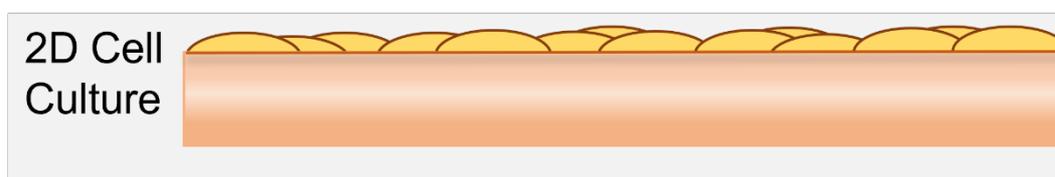
Figure 2-1. An illustration of cells cultured in 2D. The contact area between media and cells is confined to one side of the cells as they are polarized on the substrate [16].

However, even if there have been numerous studies dedicated to cellular growth mechanisms and pathogenesis, there are still aspects that are unclear about the real environment inside the tissues. The essential functions such as response to external stimuli, cell-to-cell interaction, and gene/protein signaling to be named, are happening due to the growth and arrangement of cells in a three-dimensional (3D) format and the fact that cells align themselves with their surface area in an elliptical shape and interaction with other cells [19]. Hence, even though 2D culture has proved to be useful, but still, cannot reflect the 3D environment that cells are experiencing in vivo [22, 8]. This deficiency results in many issues regarding the functionality of the cell which are described as follows:

1. Since the cell has access to only a portion of the solution, the cell's exposure to the chemical gradient is limited [22].

2. Cell function can be affected due to the forces on the cell for the accommodation of the new confined geometry which makes a polarity shift within the cell [22, 27].

3. In vivo, cells have a discrete attachment, while in the 2D culture, the attachment of the cell is limited to a continuing surface [8].

4. Since the roughness of the surface is low, it allows the cells to migrate and proliferate without any prevention, and that is not an accurate reflection of what cells are experiencing in vivo [8].

These complications mentioned above are optimized when cells are in the body because cells are in interaction with an overly complicated extracellular matrix (ECM) considering their type and location in the body. The interest in 3D cell culture increased because researchers were looking for developing platforms with better capability of representing in vivo environments [28, 29]. An opportunity for cells to grow omni-directionally is provided by the 3D cell culture platform versus the 2D cell culture that restricts them to the planar surface [8].

As it's been discussed before, 2D culture does not mimic intrinsic physiological conditions. Hence, to fill these gaps, the utilization of 3D cell culture systems at this end makes a bridge [30]. In the following subject, a comparison between these two methods has been made.

2.1.1   3D vs 2D Cell Culture

In the context of making any comparison between 2D and 3D culture, several features make variations in the effectiveness of these methods: namely the phenotype, metabolic activity, cellular functionality, and morphology. Table 2-1 and Table 2-2 are brief descriptions of differences between 2D and 3D cell culture functionalities.

Table 2-1. Effectiveness of 2D vs 3D methods in different features.

Features	2D	3D
Morphology **[20, 31]**	Flat morphology for cells The average thickness of around 3 μm Changes in morphology can not be recognized	Elliptical morphology for cells The average dimension of around ~10-30 μm Changes in morphology can be recognized
Differentiation **[32]**	Inefficient differentiation prediction	Efficient differentiation prediction Enhanced in vivo relevance
Viability **[33]**	Less viability since the interaction between cells is not well provided	High viability due to interaction between cells in 3D cell culture
Response to Stimuli **[34]**	In response to multiple sorts of stimuli that are triggered either by external factors or adjacent cells the sensitivity and morphology changes of cells are affected	In response to multiple sorts of stimuli that are triggered either by external factors or adjacent cells the sensitivity and morphology changes of cells are affected
Drug Metabolism **[35]**	Less distinguishment in different cytotoxicity in response to various drugs like doxorubicin, vinorelbine, and paclitaxel	Enhancement in distinguishment of cells' drug metabolization and metabolic discharge of products
In vivo Relevance **[36]**	Lack of information regarding cell-cell interactions	Providing greater intercellular interactions in results of the better-mimicked microenvironment

Table 2-2. Effectiveness of 2D vs 3D methods in different features (Table 2-1 continued).

Features	2D	3D
Proliferation [20, 37, 38, 39]	-	Increase in the growth rate of many cell lines such as osteosarcoma cells, mesenchymal stem cells, tumor epithelial cells (TEC) cells, human glioblastoma cells, and human umbilical vein endothelial cells (HUVEC). However, some other cells reflected a decrease in their proliferation. Breast cancer, rat anterior tibialis muscle, sheep bone marrow, human neuroblastoma, and airway smooth muscle cells due to variations in morphology, fundamental proliferation, and expression of contractile protein showed a decrease in their growth rate

2.1.2   Methods of 3D Cell Culture

Several methods for the 3D cell culture have been reported by researchers so far and each has its advantages and drawbacks: The hanging-drop method, forced-floating method, matrices and scaffolds, and agitation-based approaches are a few to be named [20]. Table 2-3 and Table 2-4 describe a summary of each method.

Table 2-3. Description of conventional methods for 3D cell culture.

Conventional methods for 3D cell culture [20, 28, 40, 41, 42].	Properties
Hanging drop Cells in suspension Cell spheroid	One of the most reliable methods, Easy-to-execute, The concentration of cells happens at the tip of the drop [20] Cells are overall homogenous in morphology [43] Easy access to the cultured spheroids to harvest them [44]
Forced floating Central fusion Non adhesive coating	Providing firm and consistent spheroids Promotion of cell-cell interaction [45] Adhesion of cells is prevented using coating techniques [45, 46, 47]
Matrices and scaffolds Growth factors	Extra Cellular Matrix (ECM) is utilized to culture, embed, and grow the cells either within the gel or on top of the gel [48] ECM provides better cell-cell interaction and communication with each other [49, 50]
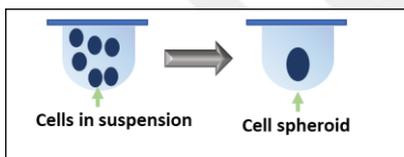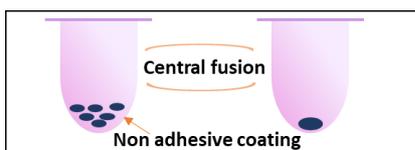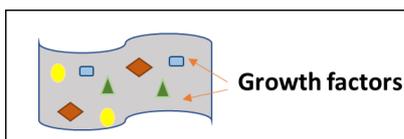
Table 2-4. Description of conventional methods for 3D cell culture (Table 2-3 continued).

Conventional methods for 3D cell culture	Properties
Other approaches	A motion to the cell is provided using a moderate rotation stirring which prohibits cells from adhesion to walls and making cell-cell interaction [20]
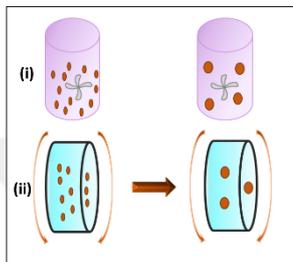
2.2 Microfluidic-Based 3D Cell Culture

Since microfluidic emerged in the 1990s An advanced platform was offered in biological applications [51]. As microfluidic systems have been integrated with 3D culture, they brought a revolutionary improvement. Microfluidic systems provide microenvironments that resemble in vivo compatibly. Some remarkable features of this technology are as follows [20]:

- Since this system works in microscale dimensions, it matches perfectly with the cellular structure of the human body.
- To simulate the complexity and dynamic 3D network inside the human body, chemical gradients can be used.
- Because reagents are consumed in a very low amount, microfluidic systems are very low cost as they use specimens in nano-liter volumes.
- To enhance the growth situation and proliferation of cells in 3D culture, microfluidic devices are constructed with substrates that are permeable to oxygen such as silicon and biodegradable polymers.

- Microfluidics' presence claimed a multifaceted technology in which controlling and handling multiple functions namely culture, medium refilling, detachment of cells, sampling, detection of subsequent, mixing, and cell capture are possible.

- To have an ideal 3D culture platform, feeding cells for their growth and proliferation by providing the required nutrition, oxygen, and moisture should be done simultaneously with the removal of waste materials and degraded products. Microfluidic systems revolutionized the field of 3D culture by offering all those mentioned privileges at once.

2.2.1 Microfluidic-Based 3D Cell Culture Platforms

Several kinds of microfluidics are characterized based on the used substrate and the method of fabrication of micro-devices that support the establishment of their function in 3D culture methods. This means the method of fabrication and the selection of the materials should ensure the desire for the right design and integrity of the platform. Various microfluidic-based 3D cell culture platforms are discussed in the following section.

2.2.1.1 Glass-Based Platforms

These platforms are chosen when working with different organic solvents and high temperatures in the process. Nevertheless, the use of this technique is limited due to the high-cost fabrication and the need for specific types of equipment [52]. Generally, this technique is incorporated with polymers to fabricate a hybrid type of microfluidics [53, 54]. High-resolution microscopy requires developed optical characterizations in a system in which glass-based platforms offer such properties. Since this platform is capable of providing a stable surface with a well-defined boundary as well as a reproducible and solid electroosmotic flow, it is especially used in long-term research or where multiple-time actions are required [55].

14

2.2.1.2 Polymer-Based Platforms

There are various polymers utilized as biocompatible substrates such as poly methyl methacrylate (PMMA), polydimethylsiloxane (PDMS), cyclic olefin copolymers (COC), polycarbonate (PC), polyethylene terephthalate (PET), and polyimide (PI) which each have specific properties desirable in different application and can be utilized in microfabrication techniques. Among all, in polymer-based systems, PDMS as a biocompatible substrate has taken more attention due to its permeability to oxygen and cost-effectiveness [56, 57]. However, since PDMS is naturally hydrophobic, advanced surface treatments like plasma treatment or polymer grafting are the primary steps required [58]. To simplify and assist perfused 3D cell culture platforms, the use of PDMS in the fabrication of these devices has been extensive. The aim of fabricating these devices is to simulate in vivo conditions which can be obtained by device optimization to flow the medium and perfuse the oxygen through the culture areas [20].

2.2.1.3 Gel-Based Platforms

To have a better microenvironment in terms of mimicking in vivo conditions, gel-based platforms integrated with micro-technologies and cell biology enable us to develop systems like organ-on-chips (OoC). In these systems, using biochemical and biophysical signals of gels which are a combination of water, protein, and enzymes, help to mimic the natural microenvironment [59]. To analyze and investigate spatial and temporal features of several factors which regulate the differentiation of cells, some developed devices have been fabricated in which channels infused with the medium are integrated with micro-wells [60]. To fabricate microchip systems for 3D culture purposes, polymers which were originated in nature like agarose, collagens, and fibrin have been used. Using the soft lithography method to fabricate an agarose-based chip, Ling et al. cultured several cell lines comprising AML 12 and hepatocytes [61]. To do so, a cell-laden agarose replica mold with a thickness of 1

cm was fabricated, and a hot solution of agarose has been cooled to 70 °C. Afterward, a mixture of cell suspension was created. Then to make the gel, the agarose-cell mixture was spread out onto a silicon master [20]. In another work by Ling et al., for delivering vital nutrients and oxygen to cells while they are cultured in the hydrogel, they used a SU-8 mold mask on a silicon wafer to fabricate an agarose-based platform [61].

2.2.1.4 Paper-Based 3D Culture Platforms

Another platform known as paper-based microfluidic systems has been suggested by the Whitesides group after they observed the requirements of being facilitated with specific engineering knowledge and instruments in the glass-based systems and polymer-based systems [62]. Paper-based platforms are mostly favorable due to their simplicity and cost-effectiveness. Based on recent research, it's been suggested to use this platform for the proliferation activities of cancerous and endothelial cells [63]. Research related to cell migration among various cell-based assays has been done using forming 96 multilayer arrays containing cells and fabricated by Whatman filter papers [64].

2.3 Gel Confinement in Microfluidic Devices for 3D Cell Culture

Gel confinement in microfluidics extensively depends on the way that the geometrical patterning of the device ensures the confinement of the biological hydrogels [65]. In many cases where the pattern of the geometry is circular reservoirs consisting of only one inlet and one outlet, medium transportation to the chamber, may result in damaging the cells due to the high sheer force they are facing [66, 67]. Generally, using micropillars or phase guide techniques for gel confinement purposes overcomes the mentioned problem since they provide reliable control of the meniscus of liquid and air [68].

16

2.3.1   Micropillar array

A chamber with two rows of micropillar arrays was developed first by Toh et al. Fig. 2-2 is an illustration of this micropillar array chamber. In this system, 3D cell-cell and cell-matrix interaction was precisely controlled. Cells were seeded by being perfused through the micropillar arrays [69]. However, since cell immobilization depends on the flow rate, cell damage happened in some cases [70]. This platform has been adapted and used in many applications widely [71].
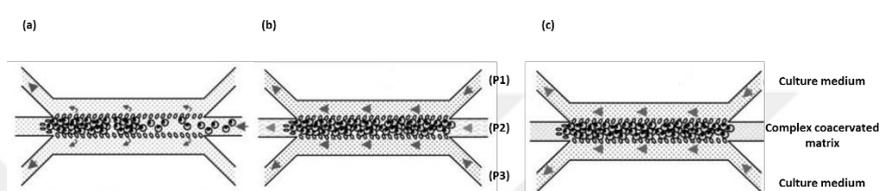
Figure 2-2. Micropillar array chamber working principle. (a) 3D immobilization by micropillar array. (b) Formation of 3D ECM support by laminar flow. (c) Removal of excess polyelectrolytes followed by perfusion culture of immobilized cells [69].

2.3.2   Phaseguides

Phaseguides have been in use over the past few decades. They are a type of barrier used in microfluidic systems to control the filling and emptying of chambers of various shapes [72]. Phaseguides are tiny ridges located at the bottom of a channel that functions as barriers to prevent the movement of fluids [73]. One advantage of phase guide microfluidic devices is that capillary pressure barriers provide precise control over the handling of liquid in terms of filing or emptying. Hence, they offer a high degree of precision and control over the manipulation of cells. These systems have become popular in recent years and have been used in various applications such as 3D cell culturing [74].

2.4   Hydrogel-Based Microfluidic platforms for Mimicking Extra Celluar Matrix Microenvironment

Cell functionality like growth and communication requires continuous control and regulation where such control is provided by Extra Cellular Matrix (ECM) in in vivo conditions [75]. The reason why ECM is essential in cell culture is that ECM is considered a substitute for the natural cell microenvironment. Hence, using it increases cell growth. The importance of ECM microfluidic 3D cell culture platforms bulleted as follows:

- Cell adhesion, immobilizing, and attachment are facilitated since ECM provides cell binding sites [76, 77].
- If the composition is maintained according to the purpose of the application, ECM may result in an improvement in gene expression in cells [78, 79].
- ECM can be used as a natural obstacle to prohibit unusual cell migration and proliferation [78].

As a perfect example of ECM, synthetic or natural hydrogel can be mentioned [80, 81] since they are hydrophilic and possess a tunable stiffness. Some examples of hydrogels are based on synthetic polymers such as polyethylene glycol (PEG), poly-N-isopropyl acrylamide (PNIPAM), polyvinyl alcohol (PVA), poly(2-hydroxyethyl methacrylate) (PHEMA), [76] or polyacrylic acid (PAA) [82]. Some hydrogels are also made from natural polymers such as fibrin, collagen, and hyaluronic acid [82]. In microfluidic devices, to directly form 3D microtissues, the mentioned hydrogels are utilized. Hydrogels have shown great proof regarding enhancements in the formation of organoids and as a result, improvement in control of the model's size, shape, and mechanical features.

CHAPTER 3

LIQUID CONFINEMENT AND CHAMBER ISOLATION IN THE CHAMBER

As 3-dimensional cell cultures are believed to have a better representation of the cell's microenvironment, microfluidic systems as a high-demand technology for 3D culture purposes, allow for developing methods that precisely can be used in cell-based assays [83, 84, 85]. For instance, various microfluidics can be developed to better recapitulate different organs' responses and functionality in their physiological environment. In this context, forming spheroids, which technically are isolated cell lines to live together in a spherical shape, is one of the most used methods. Mostly, forming spheroids comes from the suspension of cells in the hanging drop method [41], hollow microsphere [86], or a specifically designed and constructed microfluidic. In this work, the isolation of different types of cells in 3D using a micro-well-based microfluidic, roughly cylindrical shape, is proposed. The purpose is to isolate a cylindrical chamber for creating a 3D environment for cells to grow and experience a similar microenvironment as they do in vivo.

This chapter is dedicated to multiphase flows and the mechanism of chamber isolation. After modeling the design, to investigate the design optimization, the level-set method is employed on a geometry utilizing COMSOL Multiphysics ® v5.3a.

3.1   Description of The Model Geometry

In this section, a suggested design for a microfluidic-based 3D cell culture platform is discussed. This design provides a high degree of control over the isolation of microwells, using multiphase flow terminology, by demonstrating an attached well to the main channel which is supposed to be considered as an isolation section. Fig.

3-1 shows the schematic of the geometry utilized in the simulation, where the important parameters are illustrated and described in Table 3-1.
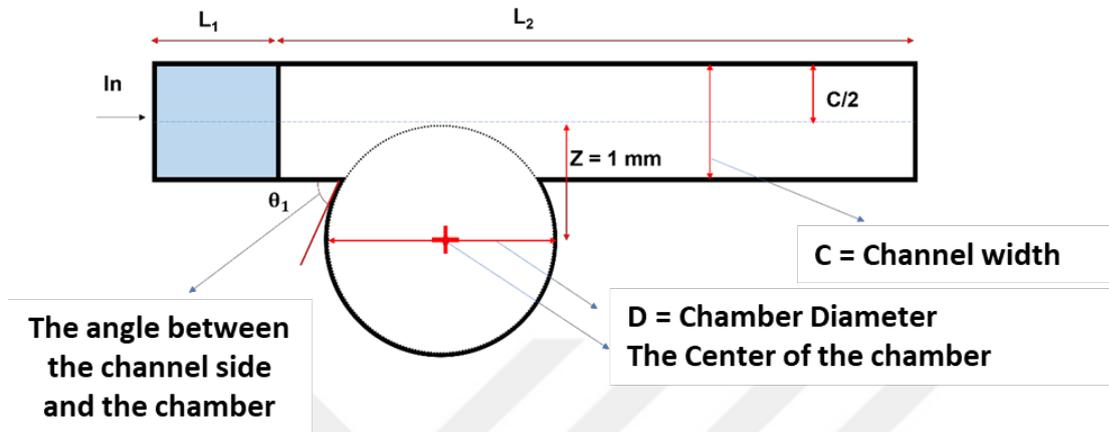
Figure 3-1. Description of the model geometry.

Table 3-1. Specification of dimensions in the design.

Parameter	Size (mm)
L_1	1
L_2	4
C	1
D	Variable (Range between [1-2])
Z	1
Depth	0.3
θ_1	(Range between [30˚-60˚])

There is a main channel which on the side of it a well is attached. The width of the channel is specified as 1 and its length is 4 mm. To show the initial value in the simulation, a square with a length of 1 mm is attached to the right side of the channel where we have inlet flow. In the simulation, this square is filled with either water or oil in each step accordingly to the initial value. The well is in the shape of a circle that its diameter is variable in the design to obtain the optimized design. The distance

between the intersection of the channel and the center of the chamber is defined as constant Z=1. In 2D simulations in COMSOL, the depth of the channel is defined as 0.3 mm. θ_1 is the angle between the channel side and the well and is one of the most important parameters in the design as it clarifies the possibility of flow inside the chambers. θ_1 ranges between 30˚ to 60˚ based on the diameter of the chamber.

The properties affecting the system include the dynamic viscosities of water (μ_w) and oil (μ_o), the densities of water (ρ_w) and oil (ρ_o), the contact angle (θ_w) between water and air and between water and oil, the applied pressure in the inlet (P_{in}), and the interfacial tension between the water-air and oil-air.

3.2   Simulation Setup Based on Boundary Conditions

To analyze the channel and chamber filling as well as chamber isolation, the fluid's properties are considered the same as the values of distilled water and oil in the parameter setup of the simulation. Some of the important parameters worth mentioning are the dynamic viscosity and density of the materials used in the simulation which are mentioned in Table 3-2. Lastly, since there is a liquid-liquid interface in the system, the surface tension force in the momentum equation is by default activated.

Table 3-2. Properties of water and oil.

Parameter	Water	Oil
Dynamic viscosity	1 mPa·s	1.24 mPa·s
Density	1000 kg/m^3	1614 kg/m^3

In this design, boundary condition settings are based on pressure inlet both for water and oil in the inlet. To provide proper conditions for the system to work properly and since this system is fully pipette-operated, the pressure in the inlet for water and oil injection needs to be at a minimum of 300 Pa. Pressure set up in the outlet is

considered as 0 Pa for both water and oil injection. The effect of pressure on the system is discussed in the next session.

To make the interface movement happens along the wall, a wetted wall condition should be considered since the walls are in contact with fluid-gas and fluid-fluid for the water-air interface and water-oil interface, respectively. In this work, the contact angle is assumed as $\theta_w = 60°$ for the water-air interface and $\theta_w = 140°$ for the water-oil interface which are shown in Fig. 3-2. The selection of contact angle in this work is according to the experimental knowledge of measuring the contact angles of water and oil on a PMMA substrate. Moreover, parameters related to meshing must be characterized with care.
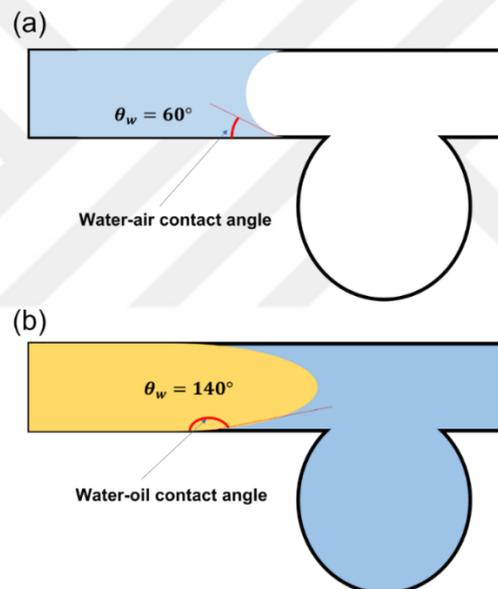
Figure 3-2. Description of contact angle in the design. (a) The contact angle between water and air. (b) The contact angle between water and oil.

3.2.1   Element Order and Discretization

In COMSOL, to solve the partial differential equations (PDE) the finite element method is utilized. The finite element method discretizes the domain by meshing it with smaller subdomains called elements.

Specific element orders are provided to be used in (PDE) and faint-form interfaces. The element order has a direct influence on the number of degrees of freeness in the solution and the precision of the solution. For instance, the shape functions for each element in the easiest sample of a one-dimensional finite element are readily a collection of polynomials described over the domain.

3.2.2 The Discretization Settings for a Physics Interface

Mostly, physics interfaces utilize Lagrange elements which contain an order of 1 to 5 or 1 to 7 in case PDE or weak form interfaces are used, in which in many cases the default discretization is set to the second order. The element orders for the physics of the model are well-aligned with the order of the numerical integration by the software. In some cases, for some of the field variables, physics interfaces utilize peculiar element types or a decreased element order.

Most of the time, the second order is set as a default discretization since the second derivation term mostly is associated with partial differential equations. Fluid flow and transport-related problems are often utilizing first-order or linear discretization by default. In specific modeling conditions, applying some changes to discretization can be encouraged. It should be noticed that even though for each physics interface variation in discretization can occur, it comes with consequences.

A decrease in discretization with no change in the number of elements provides a model which needs fewer computational actions but lacks precision. On the other hand, any increase in discretization without making any alteration in the number of elements leads to a solution with higher accuracy and with a requirement for an excellent computational resource. Using increasing the element order method to validate a model is one way, however, it is possible to approach this aim just by refining the mesh by executing a mesh refinement action since performing a discretization study on a model influences the structure of the mesh.

3.2.3   The Effect of Discretization on the Mesh

The discretization settings affect the element order of the mesh. The outcome of the discretization of mesh elements in 2D and 3D is to approximate the exact CAD geometry which is carried out by estimating the shapes associated with the boundaries of the model executing a series of geometric shape functions that resemble the exact order as the lowest discretization order utilized in each of the available physics interfaces within the model.

3.2.4   Discretization of the Fluids

To mark the choices of element order for fluid flow interfaces in the discretization of the fluid, and to demonstrate the polynomial order of the element orders the abbreviation P_mP_n is used. In this term m is a representative of the velocity components and n shows the pressure in case tetrahedral or triangular elements are utilized [87]. The associate numbers to these terms show the order of elements assigned to each. In this work, since creeping flow interfaces are used, the P2+P1 setup is applied to the modeling domain which means a second-order element for the velocity components and a linear-elements for the pressure field.

3.2.5   Building the Mesh

One of the most important steps in the COMSOL Multiphysics® after creating the geometry and allocating the physics to the model is building the mesh. The applied mesh on the model geometry in this work is shown in Fig. 3-3, and the statistics of the applied mesh in this design are described in Table 3-3.
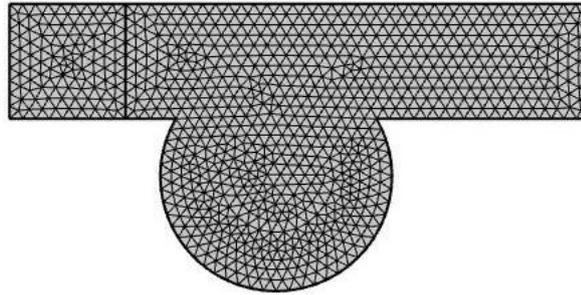
Figure 3-3. Meshing applied to the geometry modeling.

Table 3-3. Statistics of the mesh.

Statistics of a complete mesh	Statistic of domain element	Element size
Mesh vertices: 930	Number of elements: 1727	Maximum element size: 0.335
Triangles: 1727	Minimum element quality: 0.6652	Minimum element size: 0.0015
Edge element: 140	Average element quality: 0.9121	Maximum element growth rate: 1.3
Vertex elements: 12	Element area ratio: 0.3354	Curvature factor: 0.3
Quality measurement: skewness (skewness for triangles < 0.85)	Mesh area: 7.523 mm^2	Resolution of the narrow region: 1

3.3 Design Optimization

The purpose of this work and based on the model geometry shown in Fig. 3-1, is to isolate liquid in a well attached to a main channel for cytotoxicity assays. To do so, a series of two-step simulations have been carried out to obtain the optimized geometry. The two-step simulation is as follows, and Fig. 3-4 is an illustration of the work.

1. In the first step, water is injected through the inlet port and is expected to fill the whole channel and the chamber.
2. The second step is where oil is introduced to the system from the same port. As oil flows, since oil and water are immiscible, it is expected that oil does not enter the chamber and leaves the water inside the chamber isolated from the rest part of the channel.
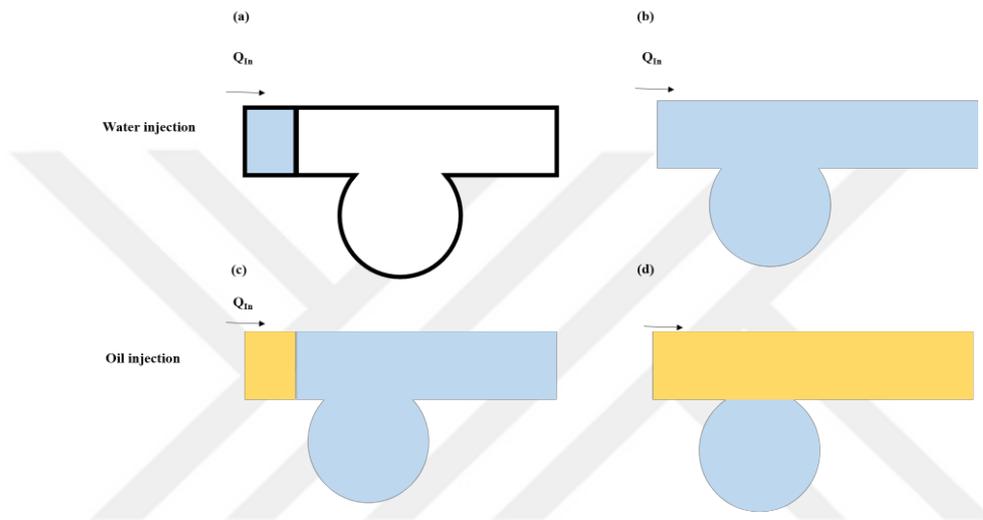
Figure 3-4. Working principle of a two-step simulation.

As it was mentioned above, the design needs to be optimized in a way that in the first step, water can fill the whole channel and chamber, and in the next step, oil injection makes the chamber isolated. For optimization, the diameter of the chambers in each design changes. Referring to Fig. 3-1 the channel width is constant in all the designs, and it is equal to one. Moreover, the distance between the intersection of the channel and the center of the chamber is equal to one and is constant in all the designs. To execute the simulations, since there is a two-step simulation, in the first step when water is filling the channel and the chamber, there is the water-air interface. Hence, the red color is an illustration of water and the blue is air. While in the second step, where there is the water-oil interface, the red color is assigned to oil and the blue color shows the water. Fig.3-5 depicts the assumptions in the simulation.
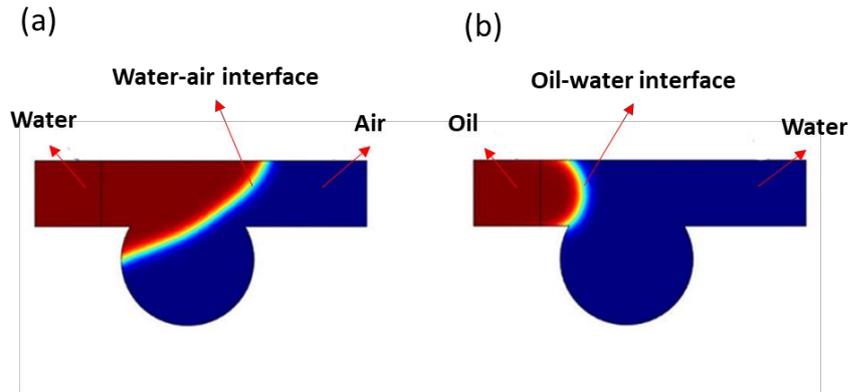
Figure 3-5. (a) Water-air interface where the red color is water and the blue is air. (b) The oil-water interface where oil is red color and water is blue.

3.3.1 The Effect of the Inlet Pressure (P_{in})

Since the boundary condition for this system is based on pressure control, the system is significantly dependent on pressure, and the pressure has a great impact on the functionality of the system. As it is shown in Table 3-4, under the inlet pressure of P_{in}= 0 Pa, neither water nor oil can flow through the channel. We constantly increased the pressure of the inlet to find the minimum value at which the system functions properly. The minimum pressure of the inlet should be set at P_{in}= 300 Pa for the system to work, and it has been set for all the designs in this work.

To show how water flows in the channel and fills the chamber as well as oil injection through the channel for chamber isolation, Table 3-5 shows a series of 5 frames, taken at different times, to show the working principle of the simulation for both two steps. The pressure inlet for this series of simulations is set as P_{in}= 300 Pa. Setting the pressure as 300 Pa is based on the experimental operation of the proposed device. Since the platform is fully pipette operated, the minimum pressure applied on the pipette tip should be 300 Pa to operate properly.

Having all said, the results of different designs are shown in Table 3-6 and Table 3-7.

Table 3-4. The functionality of the system under the pressure of $P_{in}= 0$ Pa.

Time	t = 0.0000 s	t= 0.0061 s	t= 0.0110 s	t = 0.0555 s	t = 0.1000 s
Chamber filled with water, $P_{in}= 0$ Pa					
Chamber isolation by oil, $P_{in} =0$ Pa					
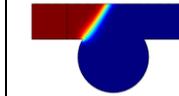
Table 3-5. Frames of different time steps taken from simulation.

Time	t= 0.0000 s	t= 0.0061 s	t= 0.0110 s	t= 0.0555 s	t = 0.1000 s
Chamber filling with water, $P_{in}= 300$ Pa					
Chamber isolation with oil, $P_{in}= 300$ Pa					
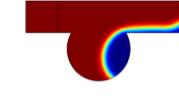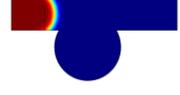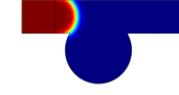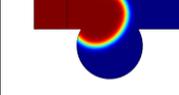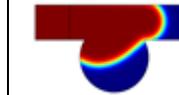
Table 3-6. The results obtained from the simulation for geometry optimization.

Chamber Diameter (mm)	Water fills the channel and the chamber which initially are occupied by air	Chamber isolation with oil
D = 1.20		
D = 1.40		
D = 1.60		
D = 1.70		
D = 1.75		
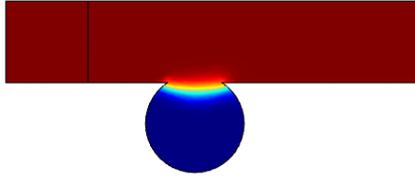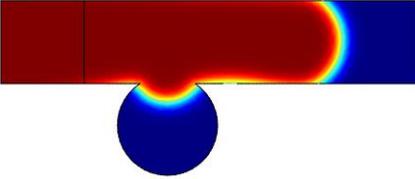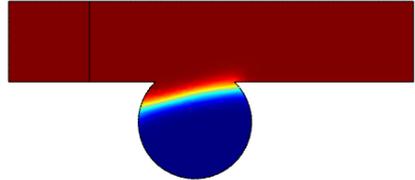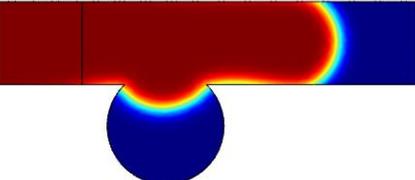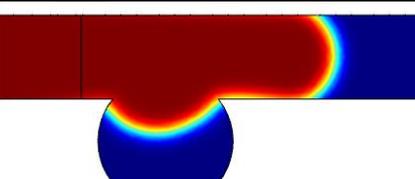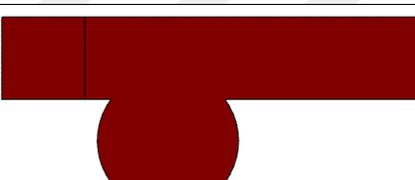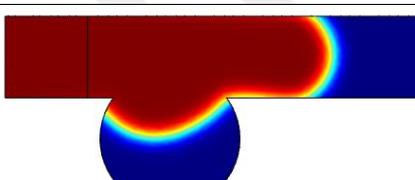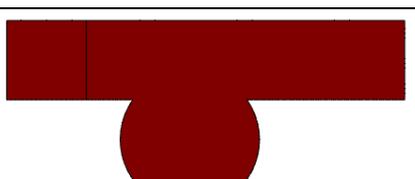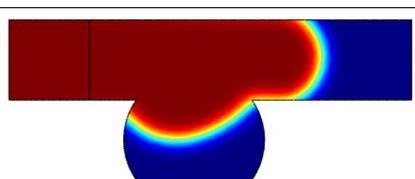
Table 3-7. The results obtained from the simulation for geometry optimization (Table 3-6 continued).
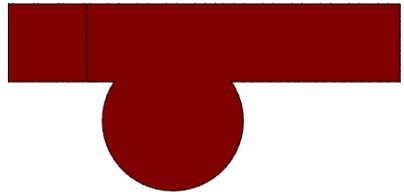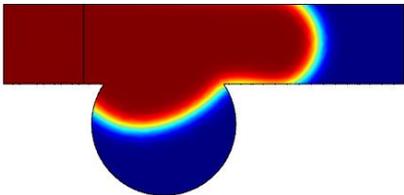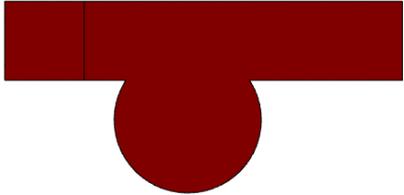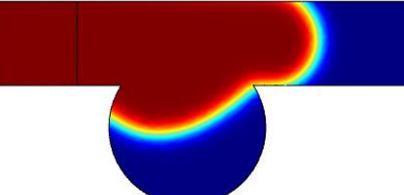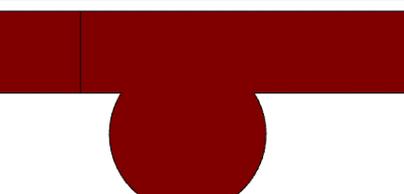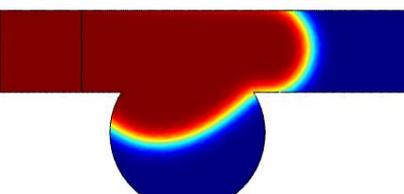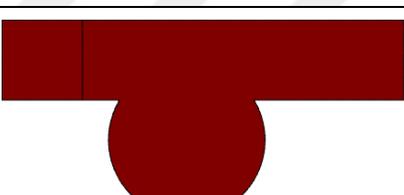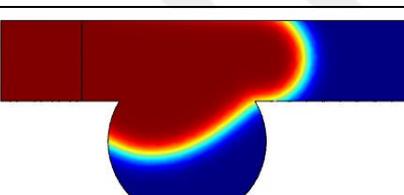
D = 1.80		
D = 1.85		
D = 1.90		
D = 1.95		
D = 2.00		
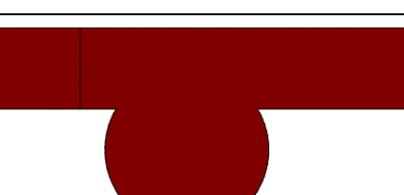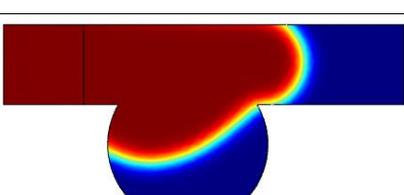
3.4 Simulation Results and Discussion

To assign a design as the optimized one, the area ratio of the water isolated in the chamber to the total area of the chamber (A) is considered as the parameter to be

compared in different designs. Equation (3.1) refers to the calculation of the area ratio. According to the results of the calculations of the area ratio shown in Fig. 3-6, it can be inferred that the area ratio inside the chambers increases by increasing the diameter of the chambers. Hence, since the area ratio in the chamber with a diameter of 2.00 mm is the highest, this design is considered the optimized one.

$$A= \frac{Area\ of\ water\ inside\ the\ chamber}{Total\ area\ of\ chamber} \tag{3.1}$$
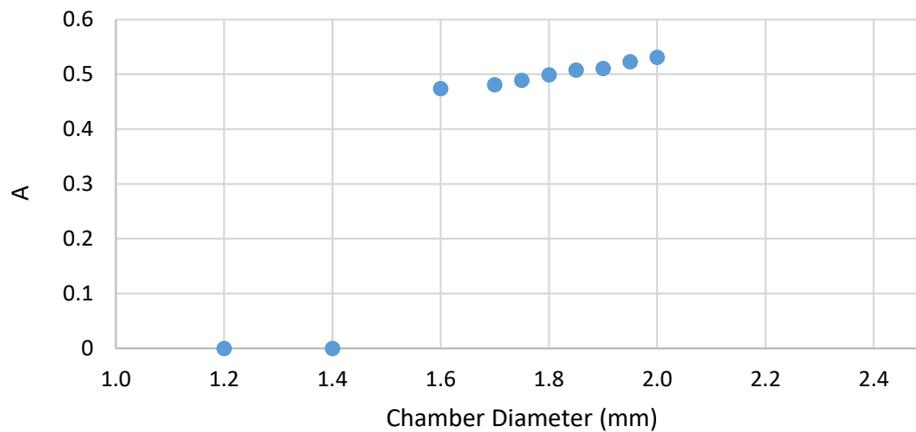
Figure 3-6. The plot of the area ratio of isolated water inside the chamber to the total area of the chamber vs the diameter of the chamber.

CHAPTER 4

MICRO-WELL-BASED MICROFLUIDIC DEVICE FABRICATION

The enhancement of microtechnology and micromachining methods has had a major impact on biomedical and biological-related applications since it brought miniature devices into action over the past few decades. Microfluidic devices can execute actions in many aspects that notably enhance the result: detection, sample separation, drug cytotoxicity assays for applications that require pretreatment and analysis, cell monitoring, and further clinical steps are a few to be named. These devices uphold many features which are huge advantages in many applications: high sensitivity, low-cost fabrication technique, the capability of executing multiple parallel tests in one set, and low material consumption. Production of these devices can be achieved using many different materials: Silicon (Si)-based materials and polymers are a few to mention. However, since silicon-based materials require surface maintenance and modification after fabrication, they may not be suitable for biological applications. Because silicon-based materials are not biocompatible, their fabrication process takes a lot of time, and they need a clean room environment in the fabrication process. Hence, development in polymer-based materials gained attention [88, 89, 90].

4.1   Polymer-Based Microfabrication Techniques

Polymer-based materials address the issues related to si-based materials since they are optically transparent, biocompatible, replicable from the production point of view, and capable of surface modification. Moreover, they offer low-cost and fast fabrication processes which are huge profits in microfabrication techniques [91]. Microfabrication techniques can make use of different types of polymers, including poly methyl methacrylate (PMMA), polydimethylsiloxane (PDMS), cyclic olefin

copolymers (COC), polycarbonate (PC), polyethylene terephthalate (PET), and polyimide (PI). Each of these polymers possesses unique characteristics that are beneficial for various applications. [88].

PMMA is highly biocompatible which makes it favorable in medical applications. The biocompatibility property of PMMA may be attributed to its resistance to stress related to temperature, chemical reactions, bioprocess, and human tissues. In this work due to the high advantage use of PMMA, it has been utilized in the fabrication process.

4.1.1   Micro Milling

Micro-milling machines can be used to pattern microchannels onto a substrate, significantly reducing the fabrication time to just a few minutes, depending on the geometry of the pattern. However, the machining of small sizes may be limited by the diameter of the milling cutters [89], which is an important consideration when using this technique [90, 91].

In this study, Fusion 360 software was utilized to design the geometry and simulate the milling process, as shown in Fig. 4-1. A 1 mm end mill was used to mill the channels and chambers, with a maximum stepdown of 0.1 mm and three passes to achieve a depth of 0.3 mm. The spindle speed and cutting feed rates were set to 4000 rpm and 20 mm/min, respectively. To mill the inlet and outlet holes, a boring technique was employed, with a 1 mm end mill selected for the task. The diameter and depth of the holes were 1 mm and 2.5 mm, respectively. The spindle speed and cutting feed rates for the boring process were set to 4000 rpm and 60 mm/min, respectively. The complete parameter set-up for milling the device is summarized in Table 4-1.
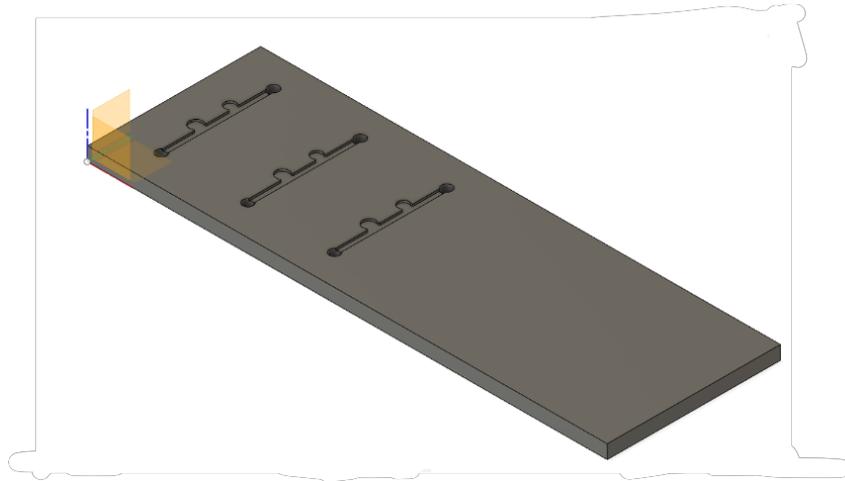
Figure 4-1. The model of geometry designed in Fusion360.

Table 4-1. Parameter indication used in Fusion360 for simulating the chip fabrication.

Parameter	Setup value
End mill diameter	1 mm
Spindle rate for channel and chamber milling	4000 rpm
The feed rate for channel and chamber milling	5 mm/min
Spindle rate for inlet and outlet drilling	4000 rpm
The feed rate for inlet and outlet drilling	5 mm/min

The machining of a PMMA substrate using CNC is shown in Fig. 4-2.

Figure 4-2. (a) Micro-milling machine and setup. (b) Processed PMMA substrate.

4.1.1.1   Solvent-Assisted Thermo-Compressive Bonding Process:

After the milling process, the processed PMMA substrate should be sealed by thermo- compressive bonding of a blank PMMA sheet. However, before applying the thermal bonding process, the surface of the substrate needs to be treated with chloroform since it is a solvent of PMMA substrates. In that sense, a solvent-treatment technique using chloroform is utilized. In this technique, there are two Petri dishes each containing 20 µL of chloroform placed in a water tank. The two sheets of PMMAs processed one and unprocessed one, are then placed on a steel separator which prevents them from direct touch with chloroform. Right after the placements, two and a half minutes is required for PMMA to get treated with chloroform vapors. After that, immediately, the two sheets are required to stick to each other, and as the result, the two PMMA sheets get bonded to each other. The evaporation process of chloroform and chemical bonding of PMMA sheets is illustrated in Fig. 4-3.
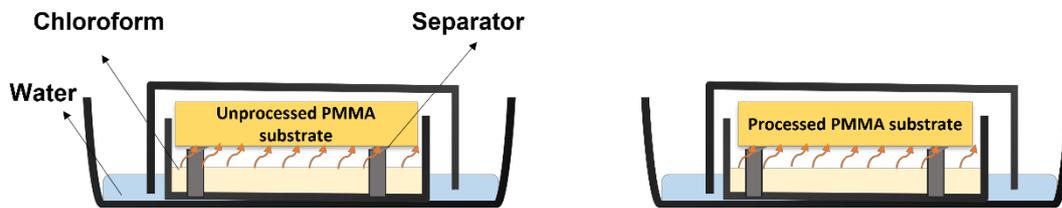
Figure 4-3. The evaporation process of chloroform and chemical bonding of PMMA sheets.

Not long after the surface treatment process thermo-compressive bonding can be applied. In this technique, a chip is placed between two silicon wafers on the heater plate. The working principle of the thermo-compressive bonding process is as follows:

1. First, the temperature of heater plates raises to around 75 °C during the first 10 minutes (T_1) of the cycle (Fig. 4-2.a),

2. Then the temperature stays steady at that temperature for about 10 more minutes (T$_2$), and for a specific amount of time, a certain force is applied to the substrate to be compressed (Fig. 4-2.b).
3. During the third period (T$_3$) temperature reduction starts until it reaches 40 °C, where the cooling process commences (Fig. 4-2.c),
4. After cooling the processed PMMA substrate and unprocessed PMMA substrate are bonded finely (Fig. 4-2.d).
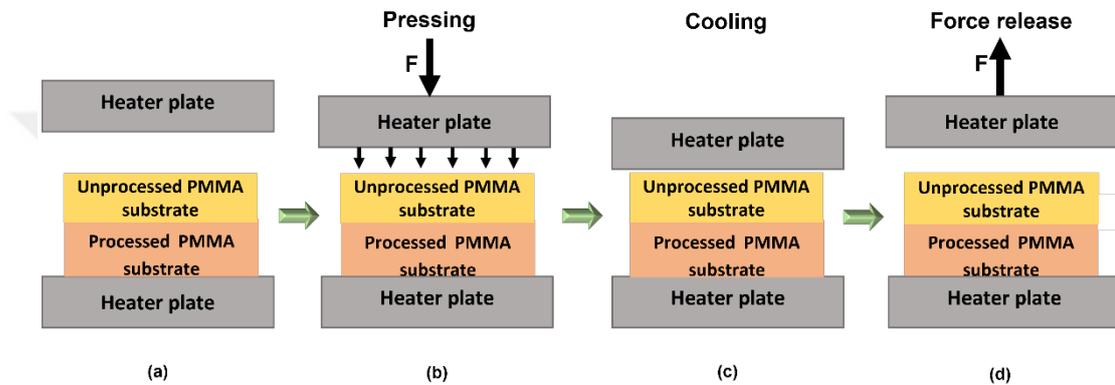
Figure 4-4. Stages of the thermo-compressive bonding process, (a) substrate placement, (b) force employment and compression, (c) cooling, (d) force release.

The cycle time of the machine is depicted in Fig. 4-3.
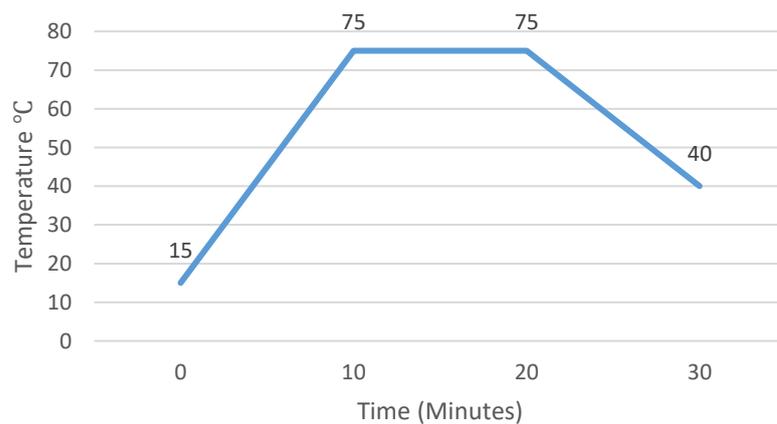
Figure 4-5. The cycle time of the thermo-compressing bonding process.

37

CHAPTER 5

EXPERIMENTAL VALIDATION OF CHAMBER ISOLATION AND LIQUID CONFINEMENT

The experiments which investigate the isolation of the chamber and liquid confinement are executed with a PMMA substrate fabricated by a milling device. The schematic of the design used in the experiments is shown in Fig. 5-1. Since the goal is to achieve the highest volume ratio of liquid confined in the chamber, the fabricated micro-well-based microfluidic contains two chambers with different diameters of the chamber (D). The chambers are placed on the sidewall of the channel in a way that the distance between the center of the chamber and the intersection of the channel (Z) is always equal to 1 mm.
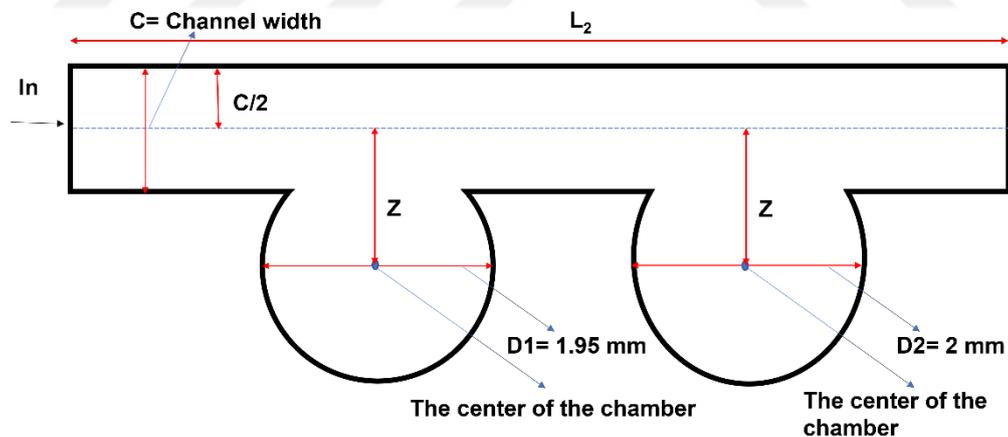
Figure 5-1. Schematic of the micro-well-based microfluidic device fabricated by PMMA.

5.1 Experimental validation of Proposed Micro-Well-Based Microfluidic regarding chamber isolation and the liquid confinement

To observe the experimental characterization of flow in the chip and to see whether chamber isolation and liquid confinement happen or not, the flow was introduced to the system using a pipette. The experimental setup of chamber isolation and liquid confinement experiments is shown in Fig. 5-2. Since the isolation of the chambers is the goal, the system requires a two-step function which is described as follows:

1. First, distilled water colored with red food dye is injected into the system through the inlet which is supposed to fill the whole channel and chamber.

2. Second, oil is inserted through the same input port to confine distilled water in the chamber and leave the chamber isolated.
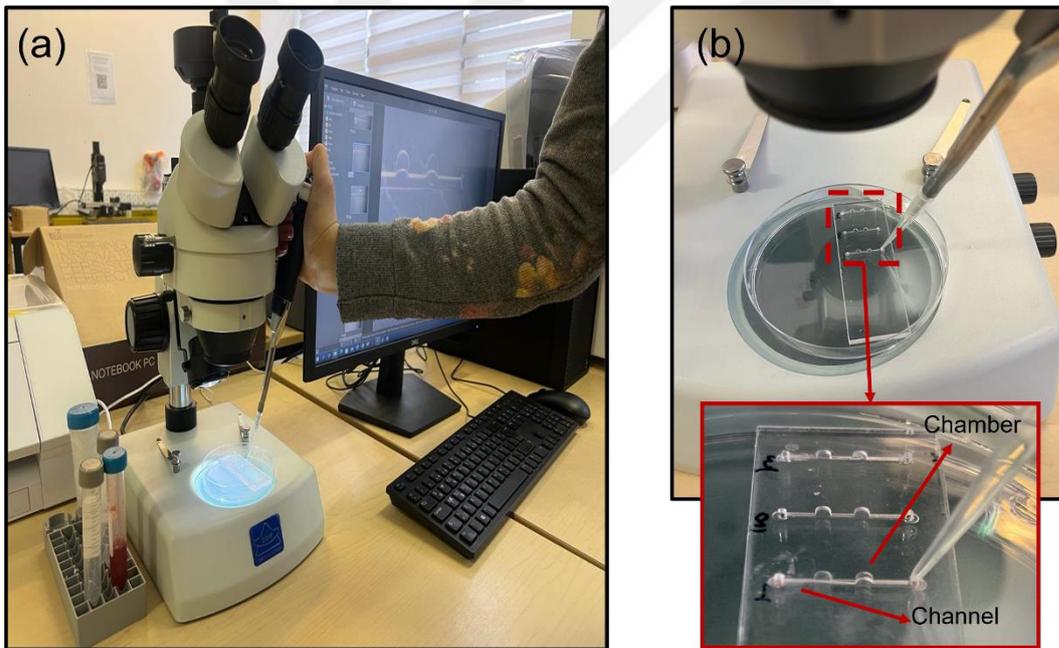
Figure 5-2. Chamber isolation experiments. (a) Experimental setup. (b). PMMA test device.

The liquid confinement in the chamber and chamber isolation were observed under the microscope and the experimental images are shown in Fig. 5-3. According to the observations, in the first step, when distilled water enters the chambers, even if there is an air bubble in each chamber it almost fills them up. In the second step, feeding the oil through the channel makes the chambers isolated while distilled water is confined in the chambers.
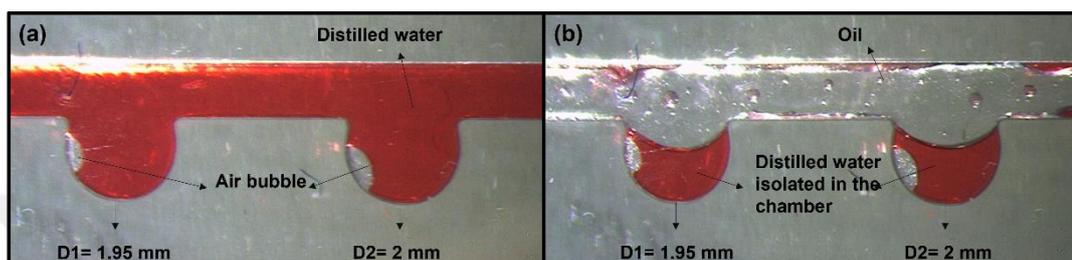
Figure 5-3. Experimental images of chamber isolation and distilled water confinement. (a) Chamber filling using distilled water. (b) Chamber isolation using oil.

The same procedure was performed to obtain the experimental characterization of flow using hydrogel and oil. Experimental images of the experiment are shown in Fig. 5-4. Based on the observation, when hydrogel flows through the channel it successfully fills the chamber with a 2 mm diameter while it fails to enter the chamber with a diameter of 1.95 mm. In the second step, inserting the oil through the channel makes the confinement of hydrogel inside the chamber and so isolation happens.
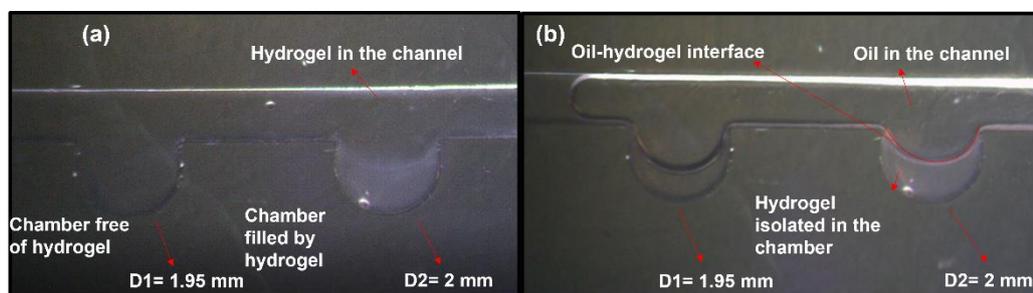
Figure 5-4. Experimental images of chamber isolation and hydrogel confinement. (a) Chamber filling using hydrogel. (b) Chamber isolation using oil.

41

The results obtained from experimental characterization of distilled water and hydrogel suggest that the system is not acting as properly as expected in terms of chamber filling and liquid confinement. This can be related to the important role of contact angle in the flow process. Hence, to solve this problem, plasma treatment of the PMMA substrate is proposed since in this way, the hydrophilicity of the substrate increases. The effect of contact angle is discussed in the following section.

5.1.1 The Effect of Contact Angle

Observations of flow characterizations of distilled water and hydrogel in the design suggest an important role of contact angle in the way that the chambers are filled. Generally, a substrate is considered as hydrophilic if the contact angle of water is less than 90°. If it goes higher than 90° we can claim the surface is hydrophobic. Plasma treatment is a way of increasing the hydrophilicity of a substrate. To observe the effect of contact angle, at first, the contact angle of water on the normal PMMA substrate is measured. Then, it is compared with a plasma-treated PMMA substrate. The PMMA substrate is treated in a vacuum chamber for 5 s. Then, the same procedure was conducted to measure the contact angle of hydrogel on a normal and plasma-treated PMMA. The results are shown in Fig. 5-5. The contact angle of 20 μL of water on a normal PMMA was measured at around 75° while it was measured at approximately 60° when a plasma treatment had been applied to the PMMA substrate. This is proof that plasma treatment increases the hydrophilicity of the PMMA substrate. Consequently, the same procedure has been proceeded for measuring the contact angle of hydrogel on the PMMA substrate. The contact angle of 20 μL of hydrogel on the normal PMMA is measured at around 60°. After applying the plasma treatment on the PMMA substrate the contact angle of the same amount of hydrogel on the plasma-treated PMMA decreased to around 45°.
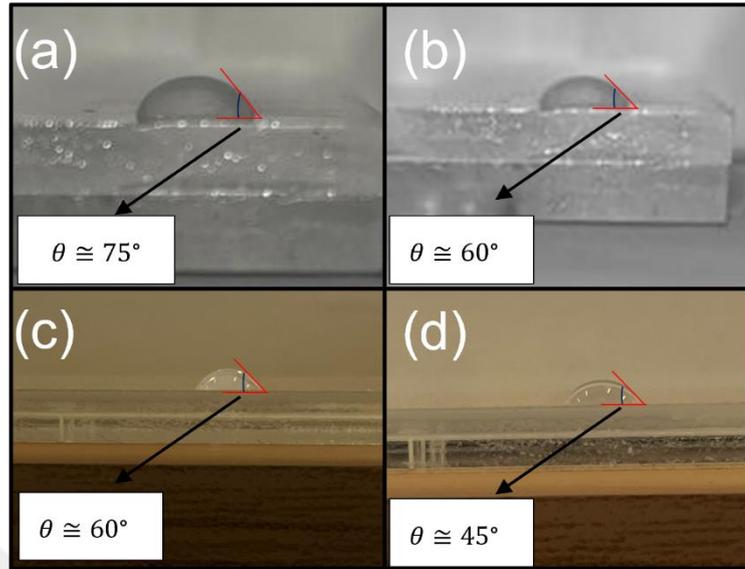
Figure 5-5. The effect of contact angle. (a) The contact angle of distilled water on a Normal PMMA. (b) The contact angle of distilled water on a plasma-treated PMMA. (c) The contact angle of hydrogel on a Normal PMMA. (d) The contact angle of hydrogel on a plasma-treated PMMA.

5.1.2　Experimental Validation of Chamber Isolation and Liquid Confinemnet on a Plasma-Treated PMMA

After treating the PMMA sheet, the flow characterization experiments were repeated to analyze the effect of contact angle. While proceeding with the experiment using distilled water, the first step was accomplished and chambers were filled with distilled water. However, in the second step, it was observed that since the hydrophilicity of the PMMA was increased after plasma treatment, injecting oil through the inlet flushed the distilled water inside each chamber away. The results are shown in Fig. 5-6.
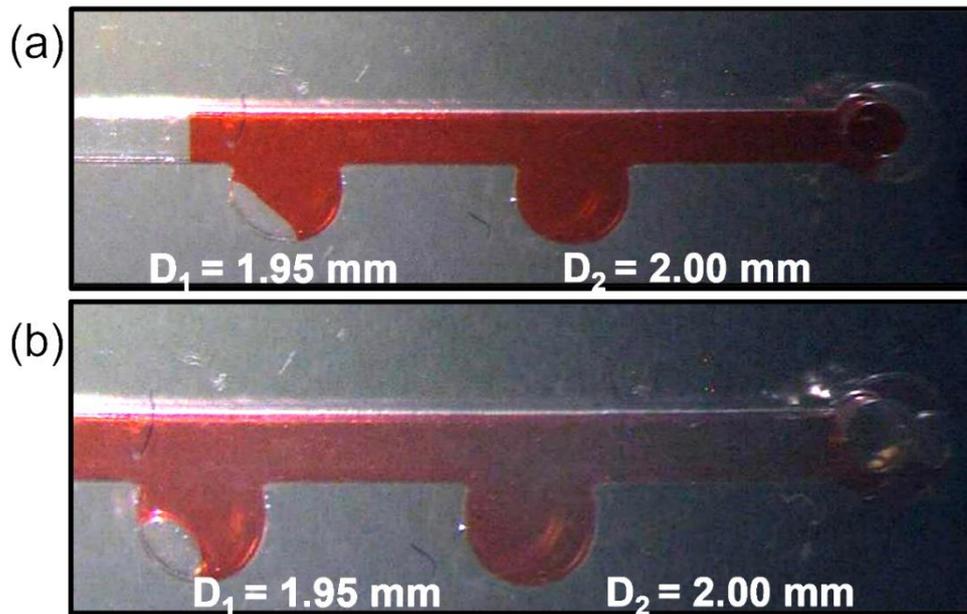
Figure 5-6. Flow characterization experiments on plasm-treated PMMA. (a) water filling the chambers. (b) oil flushing the water inside the chambers away.

During the experiment, it was realized that vacuuming the channel after introducing distilled water, makes the isolation happen perfectly. It was an improvement regarding the working principle of the chip. Hence, isolation experiments using pressure control and vacuuming the chamber were tested. The results of this experiment showed that chambers could be isolated using this technique rather than using oil. Fig. 5-7 demonstrates the results of this experiment.
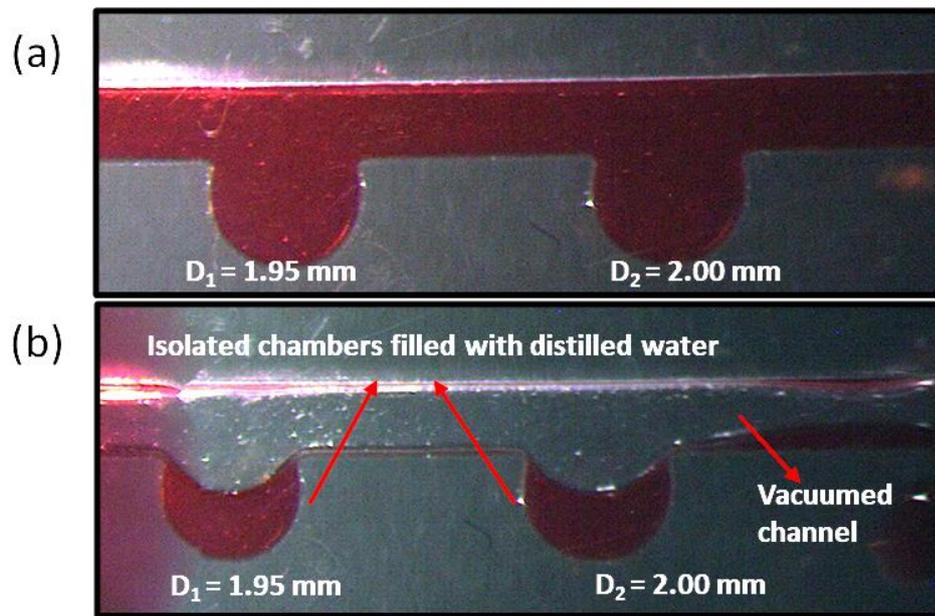
Figure 5-7. Flow characterization for distilled water and chamber isolation experiments on plasm-treated PMMA using pressure control and channel vacuuming. (a) distilled water filling the chambers. (b) vacuuming the pressure inside the channel makes chamber isolation happen.

To confirm the technique, the process was performed on a plasma-treated PMMA using hydrogel. Increasing the hydrophilicity of PMMA had a positive effect regarding the chamber filling with hydrogel. Moreover, the pressure control technique was prospering and chambers were isolated after vacuuming the channel. The result of the process is shown in Fig. 5-8.
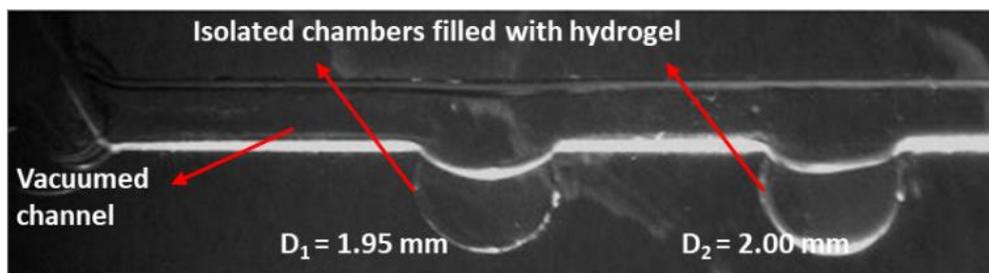
Figure 5-8. Hydrogel confinement and chamber isolation using pressure control and channel vacuuming.

5.1.3 Experimental Validation of Chamber Isolation and Liquid Confinemnet on a Plasma-Treated PMMA Using Red Fluorescent Protein (RFP) MCF-7-Laden 3D Collagen Matrix

This series of experiments were executed to gain information regarding the suitability of the suggested platform for cell culture activities. In this context, culture experiments were carried out using a breast cancer (MCF-7) cell-laden 3D collagen matrix where Red Fluorescent Protein (RFP)-MCF-7 cells have been used. Using RFP-MCF-7 cells enables us to monitor the proliferation of the cells as well as cell viability. In these experiments, three chips each containing three channels were tested with RFP-MCF-7 cells and doxorubicin anticancer drug, respectively. A dye-based live-dead assay was used to observe the viability of the cells during the experiment. Thus, Hoechst 33342 (blue fluorescence) and Propidium iodide (red fluorescence) were added to the suspension for the observation of live and dead cells, respectively. Each channel on each chamber is associated with a specific group namely as control, treated with 1 µM doxorubicin, and treated with 10 µM doxorubicin. Fig. 5-9 shows the operation principle and the structure of each three chips.
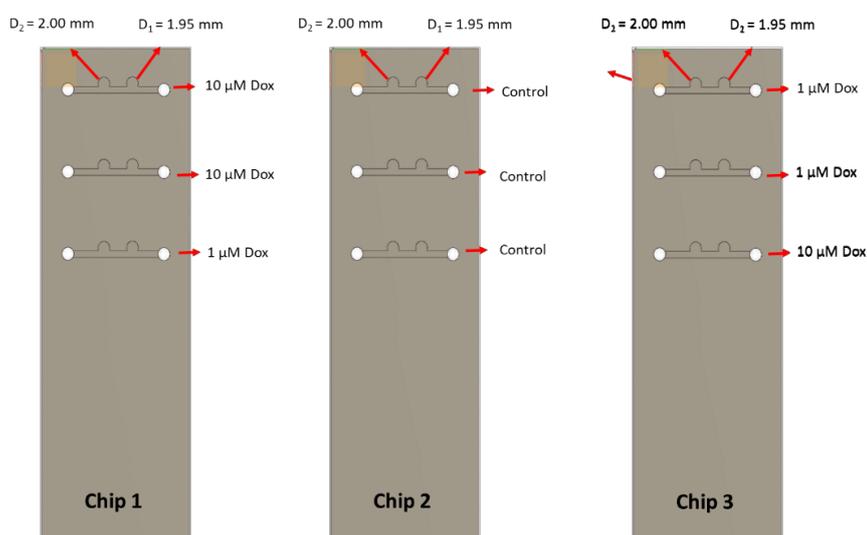
Figure 5-9. The operation principle and the structure of the chips were tested with RFP-MCF-7 Cells and doxorubicin anticancer drug.

The process was performed in a total of 48 hours. Table. 5-1 depicts the timeline of the process.

Table 5-1. Timeline of the cell culture experiments.

Timeline (hours)	Process
0 hrs	Loading the chips and taking microscopic pictures before polymerization
1 hrs	Polymerization and taking microscopic pictures after medium injection
25 hrs	Drug treatment
48 hrs	Cell viability test

To load the chips, 1ml of collagen consisting of 1×10^6 MCF-7 cells/ml was prepared. Approximately, 1 μl cell suspension containing 1×10^6 MCF-7 cells/ml were isolated in each chamber. After loading, chips were put in the incubator for one hour to let polymerization happen. After polymerization, cells were fed with fresh medium for the first 24 hours of the experiment. The setup of loading the medium is illustrated in Fig. 5-10. This 24 hours of the experiment is considered the cell growth period.
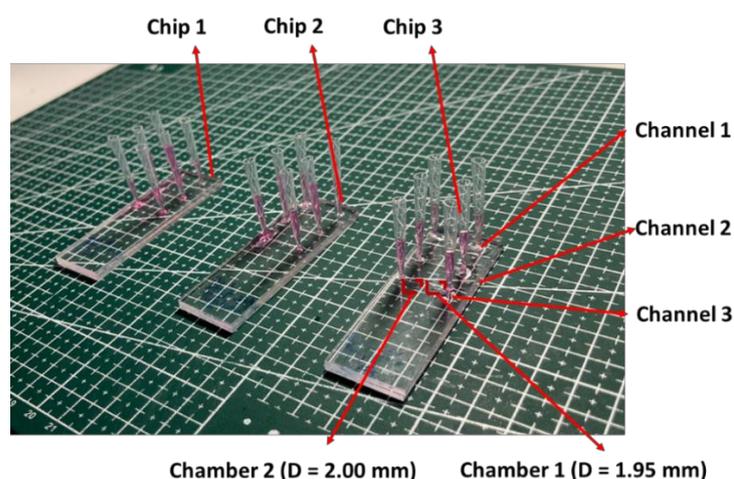
Figure 5-10. The setup for loading the medium.

To avoid medium evaporation, chips were placed into a plastic-based container and then placed into an incubator where the temperature is set to 37 ℃ which is the suitable temperature for cells to grow. After 24 hours, cells in chambers associated with drug treatment were exposed to different dosages of doxorubicin. For this purpose, doxorubicin in 2 different dosages was prepared. The preparation method is as follows:

- To prepare the main stock, 10.87 mg of Doxorubicin was used. The solution consists of 10 mM of doxorubicin in 2 mL of Medium. Equation (5.1) refers to the calculation of main stock preparation.

$$10.87 \text{ mg} = 10 \text{ mM} \times 2 \text{ mL} \times \text{molecular weight (543.52)} \qquad (5.1)$$

- To prepare 10 μM of doxorubicin in 2 mL of the medium 2 μL of the main stock was taken and diluted in 1.8 mL of medium (5.2).

$$10 \text{ mM} \times 10 \text{ μL} = 10 \text{ μM} \times 2 \text{ mL} \qquad (5.2)$$

- For 1 μM concentration of doxorubicin in 2 mL of the medium, 200 μL of 10 μM solution was added to 1.8 mL of medium to gain 1 μM concentration in a total of 2 mL solution (5.3).

$$10 \text{ μM} \times 200 \text{ mL} = 1 \text{ μM} \times 2 \text{ mL} \qquad (5.3)$$

After drug treatment, chips were placed into the incubator for another 24 hours. This 24-hour is considered the time that drugs affect the cells. After this period, to analyze the cell viability, a dye-based live-dead assay was used to observe the viability of the cells during the experiment. Thus, Hoechst 33342 (blue fluorescence) and Propidium iodide (red fluorescence) were added to the suspension for the observation of live and dead cells, respectively. Hoechst 33342 stock is supposed to penetrate all the cells, and Propidium iodide just penetrates dead cells. The solution was prepared as it is described below:

- Hoechst 33342 stock solution: 5mg/mL in dH$_2$O
- Propidium iodide stock solution: 1 mg/mL in dH$_2$O
- A staining solution with the suspension of 10 μL of Hoechst 33342 and 25 μL of Propidium iodide stock in 5 mL of culture medium was prepared.

After each specific step during the experiment, microscopic pictures, in different Z-positions, were taken to analyze the cell's functionality within 48 hours of the experiment. Pictures of each chamber in different z-positions were projected at the Z level to obtain one stack picture showing cells in the whole chamber. To analyze the cell growth during the first 24 hours of the experiment weka segmentation technique in the Fiji program has been used where cells were classified as group one and anything rather than cells as group two. The total area of cells on day-0 and day-1 of the experiment were compared to each other as the variable showing increase or decrease in cell growth. The same procedure has been done on day-2 of the experiment after exposing the chemicals to the cells to see the effect of the drugs and analyze the viability of cells in each chamber. According to the results obtained from total area calculation based on the intensity that cells are showing in each chamber, it can be inferred that cells have died in chip #1 since the total calculated area of cells following the intensity of cells in pictures taken in day-1 compared to pictures taken in day-0 of the experiment are decreased. However, chip #2 and chip #3 show a slight increase in the intensity of cells as well as the total calculated area of cells inside each chamber when comparing day-0 with day-1 of the experiment. In this series of experiments, as it is shown in Fig. 5-9, chip #2 is our control while chip #1 and chip #2 are associated with drug treatments. Analyzing of cells in chip #1 was stopped in this stage because after drug treatment there is no way to distinguish whether cells are dead because of drugs or any other reasons. After passing 24 hours of drug exposure to chip #3 and keeping chip #2 as the control group, there was a distinguishable decrease in the intensity of cells in chip #3 where cells in Channel1_Chamber1 (1.95 mm), Channel1_Chamber2 (2.00 mm), Channel2_Chamber1 (1.95 mm), Channel2_Chamber2 (2.00 mm) were treated with 1 μM and cells in Channel3_Chamber1 (1.95 mm), Channel3_Chamber2 (2.00 mm) were treated with 10 μM doxorubicin. Meanwhile, the intensity of cells in chip #2 was slightly increased. The results regarding the analysis of cell viability for control and treated cells are shown in Fig. 5-11. Appendices (A-G) refer to the information regarding the analysis of cells in different chambers on different chips.
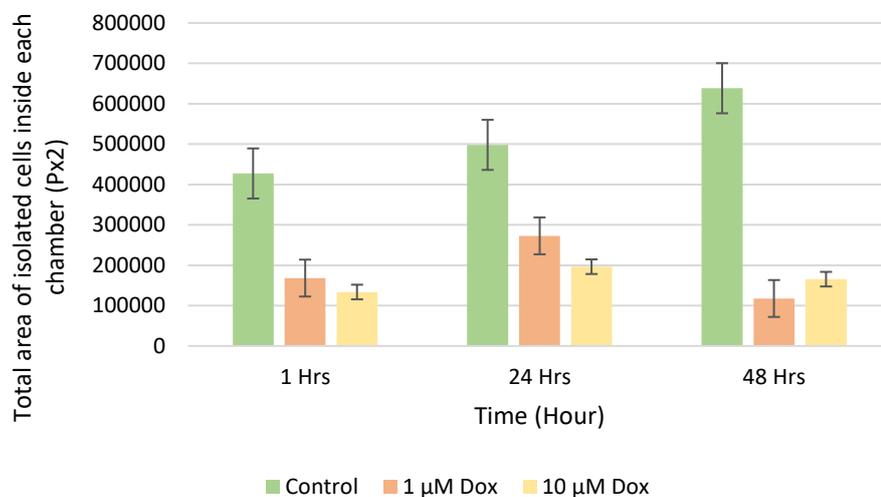
Figure 5-11. Analysis of RFP-MCF-7 cells viability for control and treated cells in a total of 48 hours.

5.1.4 Experimental Validation of Chamber Isolation and Liquid Confinemnet on a Plasma-Treated PMMA Using Wild-Type MCF-7-Laden 3D Collagen Matrix

This experiment was carried on to obtain a better estimate of cell viability tests. The procedure of this set of experiments is as exact as RFP-MCF-7 cells except for the type of cells. For this experiment, wild-type MCF-7 cells were utilized. The results are shown in Fig. 5-12. According to what has been observed from Bright-field (BF) microscopic pictures, it can be stated that the morphology and number of cells during the first 24 hours of the experiment have changed. After drug treatment and performing the viability tests, it can be concluded that after exposure, the number of dead cells (red fluorescent) has increased.
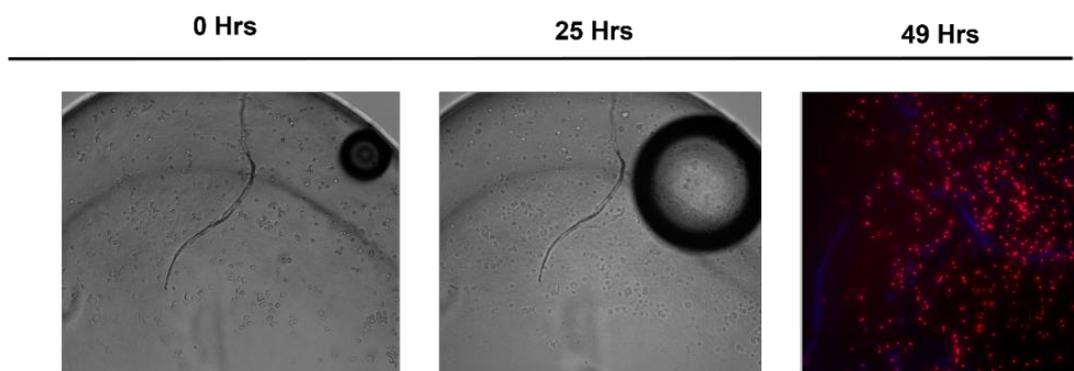
Figure 5-12. Analysis of wild-type MCF-7 cells viability for control and treated cells in a total of 48 hours.

CHAPTER 6

DISCUSSION AND CONCLUSION

This thesis encompasses the complete process of designing, fabricating, and testing a micro-well-based microfluidic 3D cell culture system for conducting cytotoxicity assays. The primary goal of this platform is to enable chamber isolation and liquid confinement, thereby providing an improved microenvironment for cell culture and analysis. To validate the efficacy of the design, it has been fabricated and experimentally tested. This chapter presents a summary of the key findings and essential discoveries of the work, along with a brief overview of the possible future directions of the research.

6.1   Accomplished Tasks

A summary of the accomplished tasks during the research is described as follows:

- This work presents a fully pipette-operated microfluidic device that is made of thermoplastic substrates and thus provides scalable manufacturing.

- An optimized design of a fully pipette-operated micro-well-based microfluid platform is proposed using Finite Element Analysis (FEA) method. Based on the results obtained from Finite Element Analysis (FEA) simulations, a circle-shaped chamber, with a 2 mm diameter, placed at the intersection of the width of the rectangle-shaped channel, demonstrates the highest volume ratio of liquid confinement in the chamber. The chamber isolation is verified by applying a two-step level-set capillary flow simulation. In the first step, water is introduced through the inlet port and fills the channel and chamber on the side wall of the

channel, and in the second step, oil injection through the same inlet port makes the water confinement in the chamber and chamber isolation happen.

- A detailed fabrication process is presented, and the chip's functionality is demonstrated through experimental results on flow characterization of distilled water and hydrogel, liquid confinement, and chamber isolation. The experimental validation shows that the chamber effectively confines distilled water and hydrogel while being isolated from the rest of the channel.

- To prove the concept of cell culture and cytotoxicity assay, RFP-MCF-7 cell-Layden 3D collagen matrix as well as wild-type MCF-7 cells were confined in isolated chambers. In a total of 48 hours experiment, cells show slight changes in morphology and growth in the first 24 hours of the process. After drug treatment, while some chambers were kept as a control group without drug treatment, some other chambers were exposed to 1 µM and 10 µM doxorubicin, respectively.

- Viability tests using a dye-based live-dead assay of Hoechst 33342 (blue fluorescence) and Propidium iodide (red fluorescence) showed a decrease in the intensity of cells inside each chamber as well as the total area of cells which illustrates the death of cells after drug treatment.

- Cell culture experiments were executed for 96 hours in total as well. However, results showed an increase in the number of dead cells after 24 hours. Hence, the duration of the experiment was decreased to 48 hours in total. Even though the results obtained in this series of experiments somehow proved the suitability of the suggested device for cell culture, still they can not be totally reliable. There should be many other considerations applied to the system to improve its functionality. For example, the reasons behind the death of the cells during the first 24 hours of the experiment in chip #1 where cells are supposed to show growth in the chambers, should be discussed. There may be many reasons for the chip not supporting cell cultures, such as inadequate culture media supply, failure to remove chemical contamination that may be introduced during manufacturing steps where chemical (APTES) treatment for membrane bonding

would cause cytotoxicity and the devices needed to be thoroughly washed (e.g. overnight with ethanol with syringe pump) to support cell culture. Moreover, the slight growth of cells in chip #2 and chip #3 can not prove the cell culture. Although BF microscopic images show slight changes in morphology and growth of the RFP-MCF-7 cells, changes in quantitive image analysis can be caused by very small alternations in the segmentation/thresholding of images in Fiji. It is also worth considering the fact that it is not uncommon that cell lines labeled with a fluorescent tag to have different growth rates compared to unlabeled ones. By comparing BF images of RFP-MCF-7 cells with wild-type MCF-7 cells in these experiments, under the same condition, it could be reported that RFP-MCF-7 grows somewhat slower than regular unlabeled MCF-7.

- Further experimental validation of cell treatment with certain drugs such as chemotherapeutic doxorubicin drug will be carried out after improving the proposed setup of the experiment.

6.2   Potential Future Work

6.2.1   Enhancement of the Model Geometry

Analysis of cell culture experiments suggests a possibility of the existence of a necrotic zone inside the chamber, around the distal periphery of the wall, where cells may not have sufficient access to fresh medium, nutrition, and any other external stimuli. In this case, if the medium is introduced from both sides of the chamber as it is illustrated in Fig. 6-1, a homogenous distribution may be obtained in the wells. In this case, the interface between the wells and the channels should be designed such that the gel loaded into the well via one of the channels do not drain into the other channel.
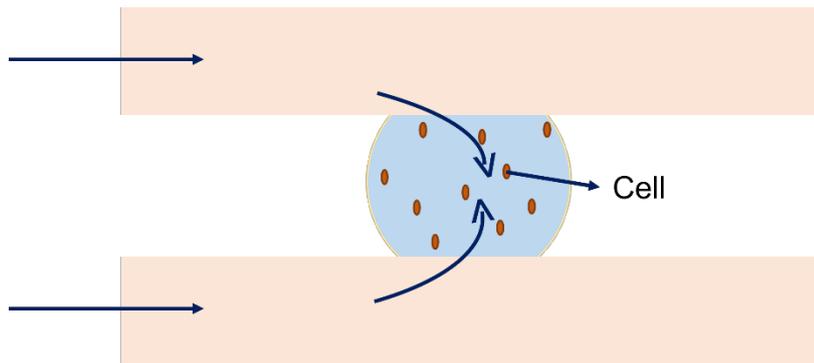
Figure 6-1. Illustration of a possible enhancement in the model geometry where injection of external stimuli occurs from two sides of the chamber.

6.2.2　　　Control of the Pressure

So far, the importance of the pressure and its effect on the device's functionality has been discussed in detail. In addition to what has been mentioned before, during the loading step of the cell-laden 3D collagen matrix, it was inferred that loading can be performed by setting a constant pressure at the minimum of 300 Pa by controlling the height of liquid while introducing it through the inlet port of the channel. Fig. 6-2 shows the suggested mechanism for loading.
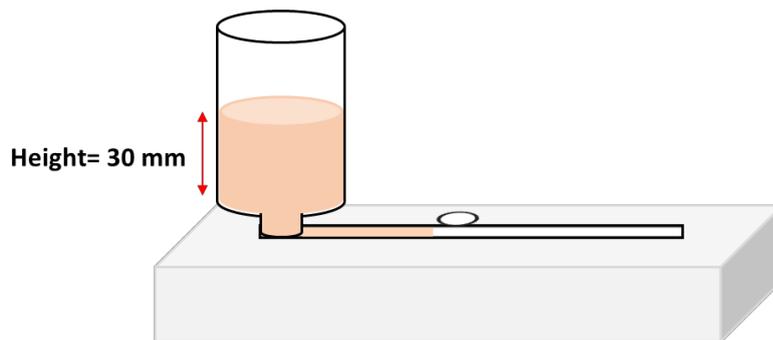
Figure 6-2. Illustration of a possible enhancement in the loading step to have better control of the pressure.

56

6.2.3 Fabrication of the Proposed Device Using Ultrasonic Embossing (UE) Technique for Scalable Manufacturing of Microfluidic Devices

As one of the objectives of this thesis is to propose a method for thermo-plastic mass production, the UE technique is taken into action. Using this technique enables us to fabricate a chip in less than 10 seconds, excluding the fabrication time of the mold. For that, an appropriate mold design is drawn in Fusion360. Since the horn of the UE machine is a circle-shaped base, the geometry of the mold is also a circle with a 20.50 mm diameter (X). The main design of the channel and chambers is the same as the previous chip. The only difference in this design is the offset of 0.75 mm (a) with a height of 0.30 mm. The offset is added for the injection molding part of the fabrication. The model of geometry designed in Fusion360 is shown in Fig. 6-3. a-c. The model was fabricated using a resin on LCD-based stereolithography (SLA) 3D printer device. The fabricated mold is shown in Fig. 6-3. d.
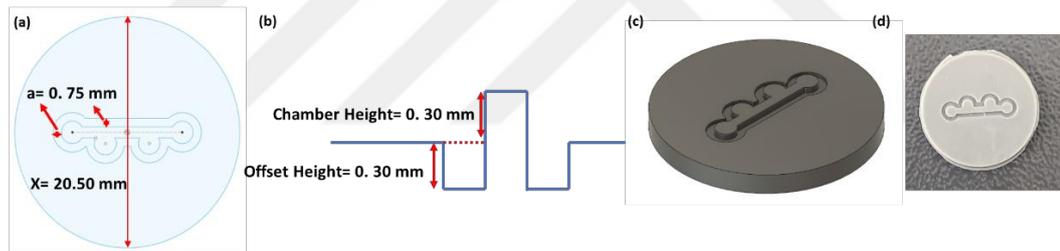
Figure 6-3. (a) Illustration of the model geometry designed in Fusion360. (b) Side-view of the model geometry. (c) 3D view of the model. (d) Fabricated mold using a 3D printer.

The machining of a PMMA substrate using UE is shown in Fig. 6-4. The purpose is to emboss the pattern of the mold on a blank PMMA sheet. Based on the experience, the vibration time is set as 1 s and the pressure applied to the PMMA sheet is 2.1 MPa. Fig. 6-5 shows the processed PMMA sheet after embossing.
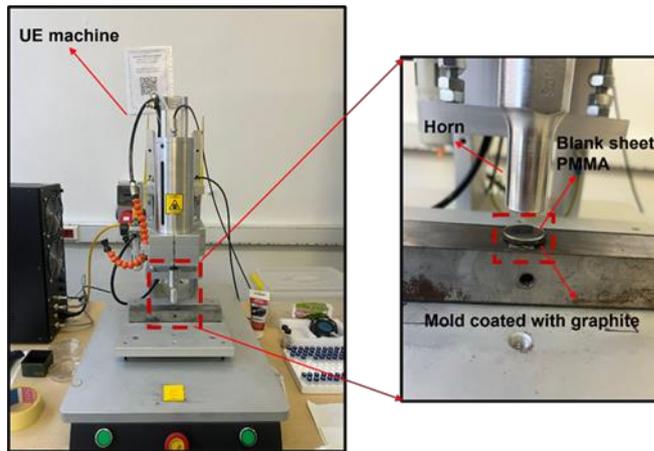
Figure 6-4. UE machine and setup.
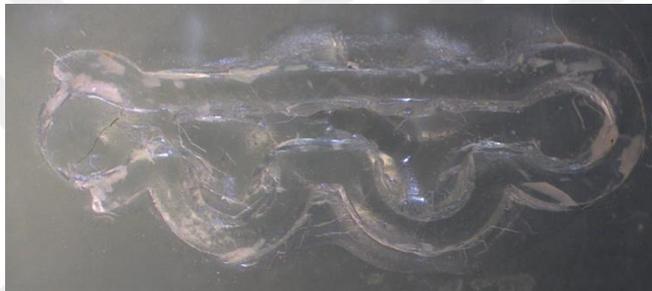
Figure 6-5. Patterning channel and chamber on a PMMA substrate using UE technique.

However, after each trial, mold deformation was observed. Hence, to prevent the deformation of the mold, in another trial it was coated with graphite during the experiment. In this specific trial, 0.7 s of vibration time and 2.52 MPa pressure were set. Fig. 6-6 shows the processed PMMA sheet after embossing.

Figure 6-6. Patterning channel and chamber on a coated PMMA substrate with graphite using UE technique.

REFERENCE

[1] B.O. Schroeder, F. Backhed, "Signals from the gut microbiota to distant organs in physiology and disease," no. https://dx.doi.org/10.1038/nm.4185, p. Nat. Med. 22, 2016.

[2] D. Yimlamai, B.H. Fowl, F.D. Camargo, "Emerging evidence on the role of the Hippo/YAP pathway in liver physiology and cancer," *Journal of Hepatology,* Vols. 63, Issue 6, pp. 1491-1501, 2015.

[3] Zhang, B., Korolj, A., Lai, B.F.L. et al., "Advances in organ-on-a-chip engineering," *Nat Rev Mater,* vol. 3, no. 2018, p. 257–278, 2018.

[4] Sackmann, Eric K and Fulton, Anna L and Beebe, David J, "The present and future role of microfluidics in biomedical research," *Nature,* vol. 507, pp. 181--189, 2014.

[5] Fang, Ye and Eglen, Richard M, "Three-dimensional cell cultures in drug discovery and development," *SLAS discovery,* vol. 22, pp. 456--472, 2017.

[6] Ware, Brenton R and Khetani, Salman R,, "Engineered liver platforms for different phases of drug development," *Trends in biotechnology,* vol. 35, pp. 172--183},, 2017.

[7] Lauschke, Volker M and Hendriks, Delilah FG and Bell, Catherine C and Andersson, Tommy B and Ingelman-Sundberg, Magnus, "Novel 3D culture systems for studies of human liver function and assessments of the hepatotoxicity of drugs and drug candidates," *Chemical research in toxicology,* vol. 29, pp. 1936--1955, 2016.

[8] Duval, Kayla and Grover, Hannah and Han, Li-Hsin and Mou, Yongchao and Pegoraro, Adrian F and Fredberg, Jeffery and Chen, Zi, "Modeling

physiological events in 2D vs. 3D cell culture," *Physiology,* vol. 32, pp. 266--277, 2017.

[9] Kapa{\l}czy{\'n}ska, Marta and Kolenda, Tomasz and Przyby{\l}a, Weronika and Zaj{\k{a}}czkowska, Maria and Teresiak, Anna and Filas, Violetta and Ibbs, Matthew and Bli{\'z}niak, Renata and {\L}uczewski, {\L}ukasz and Lamperska, Katarzyna, "2D and 3D cell cultures--a comparison of different types of cancer cell cultures," vol. 14, pp. 910--919, 2018.

[10] Sayd{\'e}, Tarek and El Hamoui, Omar and Alies, Bruno and Gaudin, Karen and Lespes, Gaetane and Battu, Serge, "Biomaterials for three-dimensional cell culture: From applications in oncology to nanotechnology," *Nanomaterials,* vol. 11, p. 481, 2021.

[11] Patra, Bishnubrata and Chen, Ying-Hua and Peng, Chien-Chung and Lin, Shiang-Chi and Lee, Chau-Hwang and Tung, Yi-Chung, "A microfluidic device for uniform-sized cell spheroids formation, culture, harvesting and flow cytometry analysis," *Biomicrofluidics,* vol. 7, p. 054114, 2013.

[12] Wu, Liz Y and Di Carlo, Dino and Lee, Luke P, "Microfluidic self-assembly of tumor spheroids for anticancer drug discovery," *Biomedical microdevices,* vol. 10, pp. 197--20, 2008.

[13] Mehta, Geeta and Hsiao, Amy Y and Ingram, Marylou and Luker, Gary D and Takayama, Shuichi, "Opportunities and challenges for use of tumor spheroids as models to test drug delivery and efficacy," *Journal of controlled release,* vol. 164, pp. 192--204, 2012.

[14] Parker, RC, "Methods of Tissue Culture, New York, Paul B," *Hoeber, Inc,* 1938.

[15] Jacoby, F and Darke, SJ, "Animal tissue culture with a synthetic medium," *Nature,* vol. 161, pp. 768--769, 1948.

[16] Castiaux, Andre D and Spence, Dana M and Martin, R Scott, "Review of 3D cell culture with analysis in microfluidic systems," *Analytical Methods,* vol. 11, pp. 4220--4232, 2019.

[17] Barnes, David and Sato, Gordon, "Serum-free cell culture: a unifying approach," *Cell,* vol. 22, pp. 649--655, 1980.

[18] Kaur, Gurvinder and Dufour, Jannette M, "Cell lines: Valuable tools or useless artifacts," *Spermatogenesis,* vol. 2, pp. 1--5, 2012.

[19] Breslin, Susan and O'Driscoll, Lorraine, "Three-dimensional cell culture: the missing link in drug discovery," *Drug discovery today,* vol. 18, p. Drug discovery today, 2013.

[20] Gupta, Nilesh and Liu, Jeffrey R and Patel, Brijeshkumar and Solomon, Deepak E and Vaidya, Bhuvaneshwar and Gupta, Vivek, "Microfluidics-based 3D cell culture models: Utility in novel drug discovery and delivery research," *Bioengineering \& Translational Medicine,* vol. 1, pp. 63--81, 2016.

[21] Stacey, Glyn, "Current developments in cell culture technology," *New Technologies for Toxicity Testing,* pp. 1--13, 2012.

[22] Kolenda, T and Kapa{\l}czy{\'n}ska, M and Przyby{\l}a, W and Zaj{\k{a}}czkowska, M and Teresiak, A and Filas, V and Ibbs, M and Bli{\'z}niak, R and {\L}uczewski, {\L} and Lamperska, K, "2D and 3D cell cultures-a comparison of different types of cancer cell cultures," *Arch Med Sci,* vol. 14, pp. 910--919, 2018.

[23] Philippeos, Christina and Hughes, Robin D and Dhawan, Anil and Mitry, Ragai R, "Introduction to cell culture," *Human Cell Culture Protocols,* pp. 1--13, 2012.

[24] Amstein, CHARLES F and Hartman, PAUL A, "Adaptation of plastic surfaces for tissue culture by glow discharge," *Journal of clinical microbiology,* vol. 2, pp. 46--54, 1975.

[25] Ramsey, WS and Hertl, W and Nowlan, ED and Binkowski, NJ, "Surface treatments and cell attachment," *In vitro,* vol. 20, pp. 802--808, 1984.

[26] Shen, Mingchao and Horbett, Thomas A, "The effects of surface chemistry and adsorbed proteins on monocyte/macrophage adhesion to chemically modified polystyrene surfaces," *Journal of Biomedical Materials Research: An Official Journal of The Society for Biomaterials, The Japanese Society for Biomaterials, and The Australian Society for Biomaterials and the Korean Society for Biomaterials,* vol. 57, pp. 336--345, 2001.

[27] Kosoff, David and Yu, Jiaquan and Suresh, Vikram and Beebe, David J and Lang, Joshua M, "Surface topography and hydrophilicity regulate macrophage phenotype in milled microfluidic systems," *Lab on a Chip,* vol. 18, pp. 3011--3017, 2018.

[28] Haycock, John W, "D cell culture: a review of current approaches and techniques," *3D cell culture: methods and protocols,* pp. 1--15, 2011.

[29] Huh, Dongeun and Hamilton, Geraldine A and Ingber, Donald E, "From 3D cell culture to organs-on-chips," *Trends in cell biology,* vol. 21, pp. 745--754, 2011.

[30] Page, Henry and Flood, Peter and Reynaud, Emmanuel G, "Three-dimensional tissue cultures: current trends and beyond," *Cell and tissue research,* vol. 352, pp. 123--131, 2013.

[31] Boxberger, Hans-J{\"u}rgen and Meyer, Thomas F, "A new method for the 3-D in vitro growth of human RT112bladder carcinoma cells using the alginate culture technique," *Biology of the Cell,* vol. 82, pp. 109--119, 1994.

[32] Farrell, E and Byrne, EM and Fischer, J and O'brien, FJ and O'connell, BC and Prendergast, PJ and Campbell, VA, "A comparison of the osteogenic potential of adult rat mesenchymal stem cells cultured in 2-D and on 3-D collagen glycosaminoglycan scaffolds," *Technology and Health Care,* vol. 15, pp. 19--31, 2007.

[33] Chen, Chunnuan and Chen, Kathryn and Yang, Shang-Tian, "Effects of three-dimensional culturing on osteosarcoma cells grown in a fibrous matrix: analyses of cell morphology, cell cycle, and apoptosis," *Biotechnology progress,* vol. 19, pp. 1574--1582, 2003.

[34] Lin, Yu-Fen and Nagasawa, Hatsumi and Peng, Yuanlin and Chuang, Eric Y and Bedford, Joel S, "Comparison of several radiation effects in human MCF10A mammary epithelial cells cultured as 2D monolayers or 3D acinar stuctures in matrigel," *Radiation research,* vol. 171, pp. 708--715, 2009.

[35] Nirmalanandhan, Victor Sanjit and Duren, Alicia and Hendricks, Peter and Vielhauer, George and Sittampalam, Gurusingham Sitta, "Activity of anticancer agents in a three-dimensional cell culture model," *Assay and drug development technologies,* vol. 8, pp. 581--590, 2010.

[36] H{\"a}rm{\"a}, Ville and Virtanen, Johannes and M{\"a}kel{\"a}, Rami and Happonen, Antti and Mpindi, John-Patrick and Knuuttila, Matias and Kohonen, Pekka and L{\"o}tj{\"o}nen, Jyrki and Kallioniemi, Olli and Nees, Matthias, "A comprehensive panel of three-dimensional models for studies of prostate cancer growth, invasion and drug responses," *PloS one,* vol. 5, p. e10431, 2010.

[37] Zhang, Xulang and Xie, Yubing and Koh, Chee Guan and James Lee, L, "A novel 3-D model for cell culture and tissue engineering," *Biomedical microdevices,* vol. 11, pp. 795--799, 2009.

[38] Chopra, V and Dinh, TV and Hannigan, EV, "Three-dimensional endothelial-tumor epithelial cell interactions in human cervical cancers," *In Vitro Cellular \& Developmental Biology-Animal,* vol. 33, pp. 432--442, 1997.

[39] Souza, Glauco R and Molina, Jennifer R and Raphael, Robert M and Ozawa, Michael G and Stark, Daniel J and Levin, Carly S and Bronk, Lawrence F and Ananta, Jeyarama S and Mandelin, Jami and Georgescu, Maria-Magdalena and others, "Three-dimensional tissue culture based on magnetic cell levitation," *Nature nanotechnology,* vol. 5, p. Nature nanotechnology, 2010.

[40] Thoma, Claudio R and Zimmermann, Miriam and Agarkova, Irina and Kelm, Jens M and Krek, Wilhelm, "3D cell culture systems modeling tumor growth determinants in cancer target discovery," *Advanced drug delivery reviews,* vol. 69, pp. 29--41, 2014.

[41] Kelm, Jens M and Timmins, Nicholas E and Brown, Catherine J and Fussenegger, Martin and Nielsen, Lars K, "Method for generation of homogeneous multicellular tumor spheroids applicable to a wide variety of cell types," *Biotechnology and bioengineering,* vol. 83, pp. 173--180, 2003.

[42] Lin, Ruei-Zhen and Chang, Hwan-You, "Recent advances in three-dimensional multicellular spheroid culture for biomedical research," *Biotechnology Journal: Healthcare Nutrition Technology,* vol. 3, pp. 1172--1184, 2008.

[43] Kurosawa, Hiroshi, "Methods for inducing embryoid body formation: in vitro differentiation system of embryonic stem cells," *Journal of bioscience and bioengineering,* vol. 103, pp. 389--398, 2007.

[44] Tung, Yi-Chung and Hsiao, Amy Y and Allen, Steven G and Torisawa, Yu-suke and Ho, Mitchell and Takayama, Shuichi, "High-throughput 3D spheroid

culture and drug testing using a 384 hanging drop array," *Analyst,* vol. 136, pp. 473--478, 2011.

[45] Ivascu, Andrea and Kubbies, Manfred, "Rapid generation of single-tumor spheroids for high-throughput cell function and toxicity analysis," *SLAS Discovery,* vol. 11, pp. 922--932, 2006.

[46] Friedrich, Juergen and Seidel, Claudia and Ebner, Reinhard and Kunz-Schughart, Leoni A, "Spheroid-based drug screen: considerations and practical approach," *Nature protocols,* vol. 4, pp. 309--324, 2009.

[47] Li, Qun and Chen, Chaoyu and Kapadia, Amit and Zhou, Qiong and Harper, Mary Kay and Schaack, Jerome and Labarbera, Daniel V, "D models of epithelial-mesenchymal transition in breast cancer metastasis: high-throughput screening assay development, validation, and pilot screen," *Journal of biomolecular screening,* vol. 16, pp. 141--154, 2011.

[48] Lee, Genee Y and Kenny, Paraic A and Lee, Eva H and Bissell, Mina J, "hree-dimensional culture models of normal and malignant breast epithelial cells," *Nature methods,* vol. 4, pp. 359--365, 2007.

[49] Kural, Mehmet Hamdi and Billiar, Kristen Lawrence, "Regulating tension in three-dimensional culture environments," *Experimental cell research,* vol. 319, pp. 2447--2459, 2013.

[50] Kleinman, Hynda K and Martin, George R, "Matrigel: basement membrane matrix with biological activity," *Seminars in cancer biology,* vol. 15, pp. 378--386, 2005.

[51] Wu, Min-Hsien and Huang, Song-Bin and Lee, Gwo-Bin, "Microfluidic cell culture systems for drug research," *Lab on a Chip,* vol. 10, pp. 939--956, 2010.

[52] Li, XiuJun and Valadez, Alejandra V and Zuo, Peng and Nie, Zhihong, "Microfluidic 3D cell culture: potential application for tissue-based bioassays," *Bioanalysis,* vol. 4, pp. 1509--1525, 2012.

[53] Shiroma, Let{\\\i}cia S and Piazzetta, Maria HO and Duarte-Junior, Gerson F and Coltro, Wendell KT and Carrilho, Emanuel and Gobbi, Angelo L and Lima, Renato S, "elf-regenerating and hybrid irreversible/reversible PDMS microfluidic devices," *Scientific reports,* vol. 6, pp. 1--12, 2016.

[54] PDMS/glass microfluidic cell culture system for cytotoxicity tests and cells passage, "PDMS/glass microfluidic cell culture system for cytotoxicity tests and cells passage," *Sensors and Actuators B: Chemical,* vol. 145, pp. 533--542, 2010.

[55] Lin Jr, Lung and Wang, Shih-Siou and Wu, Min-Hsien and Oh-Yang, Chih-Chin, "Development of an integrated microfluidic perfusion cell culture system for real-time microscopic observation of biological cells," *Sensors,* vol. 11, pp. 8395--8411, 2011.

[56] Ni, Ming and Tong, Wen Hao and Choudhury, Deepak and Rahim, Nur Aida Abdul and Iliescu, Ciprian and Yu, Hanry, "Cell culture on MEMS platforms: a review," *International journal of molecular sciences,* vol. 10, pp. 5411--5441, 2009.

[57] Sabhachandani, P and Motwani, V and Cohen, N and Sarkar, S and Torchilin, V and Konry, T, "Generation and functional assessment of 3D multicellular spheroids in droplet based microfluidics platform," *Lab on a Chip,* vol. 16, pp. 497--505, 2016.

[58] Torino, Stefania and Corrado, Brunella and Iodice, Mario and Coppola, Giuseppe, "Pdms-based microfluidic devices for cell culture," *Inventions,* vol. 3, p. 65, 2018.

[59] Russo, Maria and Cejas, Cesare M and Pitingolo, Gabriele, "Advances in microfluidic 3D cell culture for preclinical drug development," *Progress in Molecular Biology and Translational Science,* vol. 187, pp. 163--204, 2022.

[60] Gottwald E, Giselbrecht S, Augspurger C, et al.,, "Gottwald, Eric and Giselbrecht, Stefan and Augspurger, Caroline and Lahni, Brigitte and Dambrowsky, Nina and Truckenm{\"u}ller, Roman and Piotter, Volker and Gietzelt, Thomas and Wendt, Oliver and Pfleging, Wilhelm and others," *Lab on a Chip,* vol. 7, pp. 777--785, 2007.

[61] Ling, Yibo and Rubin, Jamie and Deng, Yuting and Huang, Catherine and Demirci, Utkan and Karp, Jeffrey M and Khademhosseini, Ali, "A cell-laden microfluidic hydrogel," *Lab on a Chip,* vol. 7, pp. 756--762, 2007.

[62] Derda, Ratmir and Tang, Sindy KY and Laromaine, Anna and Mosadegh, Bobak and Hong, Estrella and Mwangi, Martin and Mammoto, Akiko and Ingber, Donald E and Whitesides, George M, "Multizone paper platform for 3D cell cultures," *PloS one,* vol. 6, p. e18940, 2011.

[63] Choi, Jonghoon and Lee, Eun Kyu and Choo, Jaebum and Yuh, Junhan and Hong, Jong Wook, "Micro 3D cell culture systems for cellular behavior studies: culture matrices, devices, substrates, and in-situ sensing methods," *Biotechnology journal,* vol. 10, pp. 1682--1688, 2015.

[64] Derda, Ratmir and Laromaine, Anna and Mammoto, Akiko and Tang, Sindy KY and Mammoto, Tadanori and Ingber, Donald E and Whitesides, George M, "Proceedings of the National Academy of Sciences," *Proceedings of the National Academy of Sciences,* vol. 106, pp. 18457--18462, 2009.

[65] un-Shan, LIU and ZHANG, Yang-Yang and Zhong, WANG and Jia-Yi, DENG and Xuan, YE and Ri-Ye, XUE and Dan, GE and Zheng, XU, "esign and validation of a microfluidic chip with micropillar arrays for three-

dimensional cell culture," *Chinese Journal of Analytical Chemistry,* vol. 45, pp. 1109--1114, 2017.

[66] Lei, Kin Fong and Wu, Min-Hsien and Hsu, Che-Wei and Chen, Yi-Dao, "Real-time and non-invasive impedimetric monitoring of cell proliferation and chemosensitivity in a perfusion 3D cell culture microfluidic chip," *Biosensors and Bioelectronics,* vol. 51, pp. 16--21, 2014.

[67] Leclerc, Eric and David, B and Griscom, L and Lepioufle, Bruno and Fujii, T and Layrolle, Pierre and Legallaisa, C, "Study of osteoblastic cells in a microfluidic environment," *Biomaterials,* vol. 27, pp. 586--595, 2006.

[68] Vulto, P and Podszun, S and Meyer, P and Urban, GA, "haseguide patterns for advanced liquid handling in Lab-on-a-Chip systems," *TRANSDUCERS 2009-2009 International Solid-State Sensors, Actuators and Microsystems Conference,* pp. 409--412, 2009.

[69] Toh, Yi-Chin and Zhang, Chi and Zhang, Jing and Khong, Yuet Mei and Chang, Shi and Samper, Victor D and van Noort, Danny and Hutmacher, Dietmar W and Yu, Hanry, "A novel 3D mammalian cell perfusion-culture system in microfluidic channels," *Lab on a Chip,* vol. 7, pp. 302--309, 2007.

[70] Kim, Minseok S and Hwang, Hyundoo and Choi, Youn-Suk and Park, Je-Kyun, "Microfluidic micropillar arrays for 3D cell culture," *The Open Biotechnology Journal,* vol. 2, 2008.

[71] Yang, Kisuk and Park, Hyun-Ji and Han, Sewoon and Lee, Joan and Ko, Eunkyung and Kim, Jin and Lee, Jong Seung and Yu, Ji Hea and Song, Ki Yeong and Cheong, Eunji and others, "Recapitulation of in vivo-like paracrine signals of human mesenchymal stem cells for functional neuronal differentiation of human neural stem cells in a 3D microfluidic system," *Biomaterials,* vol. 63, pp. 177--188, 2015.

[72] Hadwen, B and Broder, GR and Morganti, D and Jacobs, A and Brown, C and Hector, JR and Kubota, Y and Morgan, Hywel, "Programmable large area digital microfluidic array with integrated droplet sensing for bioassays," *Lab on a Chip,* vol. 12, pp. 3305--3313, 2012.

[73] Yıldırım, Ender and Joore, Jos and van den Berg, Albert and Hankemeier, Thomas and Vulto, Paul, "Phaseguides as tunable passive microvalves for liquid routing in complex microfluidic networks," *LAB ON A CHIP,* p. 3334–3340, 2014.

[74] Su, Chengxun and Chuah, Yon Jin and Ong, Hong Boon and Tay, Hui Min and Dalan, Rinkoo and Hou, Han Wei, "A Facile and Scalable Hydrogel Patterning Method for Microfluidic 3D Cell Culture and Spheroid-in-Gel Culture Array," *Biosensors,* vol. 11, p. 509, 2021.

[75] Geckil, Hikmet and Xu, Feng and Zhang, Xiaohui and Moon, SangJun and Demirci, Utkan, "Engineering hydrogels as extracellular matrix mimics," *Nanomedicine,* vol. 5, pp. 469--484, 2010.

[76] Kyburz, Kyle A and Anseth, Kristi S, "Synthetic mimics of the extracellular matrix: how simple is complex enough?," *Annals of biomedical engineering,* vol. 43, pp. 489--500, 2015.

[77] Halldorsson, Skarphedinn and Lucumi, Edinson and G{\'o}mez-Sj{\"o}berg, Rafael and Fleming, Ronan MT, "Advantages and challenges of microfluidic cell culture in polydimethylsiloxane devices," *Biosensors and Bioelectronics,* vol. 63, pp. 218--231, 2015.

[78] Hoshiba, Takashi and Yamaoka, Tetsuji, "Extracellular matrix scaffolds for tissue engineering and biological research," *Royal Society of Chemistry,* pp. 1–14,, 2019.

[79] Astashkina, Anna I and Mann, Brenda K and Prestwich, Glenn D and Grainger, David W, "Comparing predictive drug nephrotoxicity biomarkers in kidney 3-D primary organoid culture and immortalized cell lines," *Biomaterials,* vol. 33, pp. 4712--4721, 2012.

[80] Huang, Guo You and Zhou, Li Hong and Zhang, Qian Cheng and Chen, Yong Mei and Sun, Wei and Xu, Feng and Lu, Tian Jian, "Microfluidic hydrogels for tissue engineering," *Biofabrication,* vol. 3, p. 012001, 2011.

[81] Khademhosseini, Ali and Langer, Robert, "Microengineered hydrogels for tissue engineering," *Biomaterials,* vol. 28, pp. 5087--5092, 2007.

[82] Castiaux, Andre D and Spence, Dana M and Martin, R Scott, "Review of 3D cell culture with analysis in microfluidic systems," *Anal Methods,,* vol. 11, pp. 4220--4232, 2019.

[83] Antoni, Delphine and Burckel, H{\'e}l{\`e}ne and Josset, Elodie and Noel, Georges, "Three-dimensional cell culture: a breakthrough in vivo," *International journal of molecular sciences,* vol. 16, pp. 5517--5527, 2015.

[84] Edmondson, Rasheena and Broglie, Jessica Jenkins and Adcock, Audrey F and Yang, Liju, "Three-dimensional cell culture systems and their applications in drug discovery and cell-based biosensors," *Assay and drug development technologies,* vol. 12, pp. 207--218, 2014.

[85] Ingber, Donald E, "Reverse engineering human pathophysiology with organs-on-chips," *Cell,* vol. 164, pp. 1105--1109, 2016.

[86] Alessandri, K{\'e}vin and Sarangi, Bibhu Ranjan and Gurchenkov, Vasily Val{\'e}r{\"\i}{\'e}vitch and Sinha, Bidisha and Kie{\ss}ling, Tobias Reinhold and Fetler, Luc and Rico, Felix and Scheuring, Simon and Lamaze, Christophe and Simon, Anthony and others, "Cellular capsules as a tool for multicellular spheroid production and for investigating the mechanics of tumor progression

in vitro," *Proceedings of the National Academy of Sciences,* vol. 110, pp. 14843--14848, 2013.

[87] Gresho, PM and Sani, RL, "Incompressible flow and the finite element method, vol 1: Advection-diffusion and isothermal laminar flow," *Journal of Fluid Mechanics,* vol. 411, pp. 378--381, 2000.

[88] Scognamiglio, Viviana and Rea, Giuseppina and Arduini, Fabiana and Palleschi, Giuseppe, "Biosensors for sustainable food-new opportunities and technical challenges," 2016.

[89] Y. Xia and G. M. Whitesides,, "Soft lithography,," Vols. vol. 28,, 1998..

[90] F. Çoğun, Numerical and experimental investigaton of ultrasonic embossing technique for fabrication of thermoplastic microfluidic devices, Ph.D. - Doctoral Program, Middle East Technical University, 2018.

[91] Duffy, David C and McDonald, J Cooper and Schueller, Olivier JA and Whitesides, George M, "Rapid prototyping of microfluidic systems in poly (dimethylsiloxane)," *Analytical chemistry,* vol. 70, pp. 4974--4984, 1998.

[92] Bang, Young-bong and Lee, Kyung-min and Oh, Seungryul, "-axis micro milling machine for machining micro parts.," *International Journal of Advanced Manufacturing Technology,* vol. 25, 2005.

[93] Wilson, Mary E and Kota, Nithyanand and Kim, YongTae and Wang, Yadong and Stolz, Donna B and LeDuc, Philip R and Ozdoganlar, O Burak, "Fabrication of circular microfluidic channels by combining mechanical micromilling and soft lithography," *Lab on a Chip,* vol. 11, pp. 1550--1555, 2011.

[94] Okagbare, Paul I and Emory, Jason M and Datta, Proyag and Goettert, Jost and Soper, Steven A, "Fabrication of a cyclic olefin copolymer planar waveguide

embedded in a multi-channel poly (methyl methacrylate) fluidic chip for evanescence excitation," *Lab on a Chip,* vol. 10, pp. 66--73, 2010.
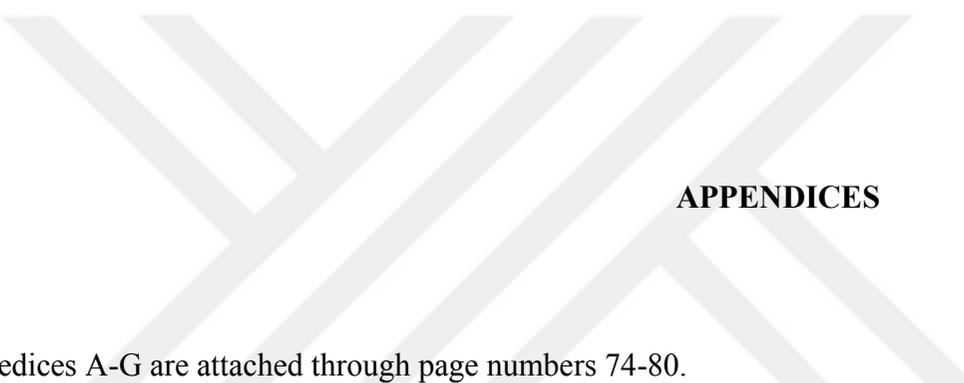
APPENDICES

Appedices A-G are attached through page numbers 74-80.

A. Cell Growth Analysis for Targeted-RFP MCF-7 Cells in Different Chambers During 48 Hours of Experiment in Chip #1.

	Chip 1											
	Channel1_Chamber1 (1.95 mm)		Channel1_Chamber2 (2.00 mm)		Channel2_Chamber1 (1.95 mm)		Channel2_Chamber2 (2.00 mm)		Channel3_Chamber1 (1.95 mm)		Channel3_Chamber2 (2.00 mm)	
	4x	10x	4x	10x	4x	10x	4x	10x	4x	10x	4x	10x
Day 0 FL												
Day 0												
Day 0 BF												
Area	49063	144127	104806	493425	71269	236056	94463	312835	77980	328528		754455
Day 1 FL												
Day 1												
Day 1 BF												
Area	23068	63054	42247	102802	24323	106219	30800	88111	19455	117514	49523	255990

74

B. Cell Growth Analysis for Targeted-RFP MCF-7 cells in Different Chambers During 48 hours of Experiment in Chip #2.

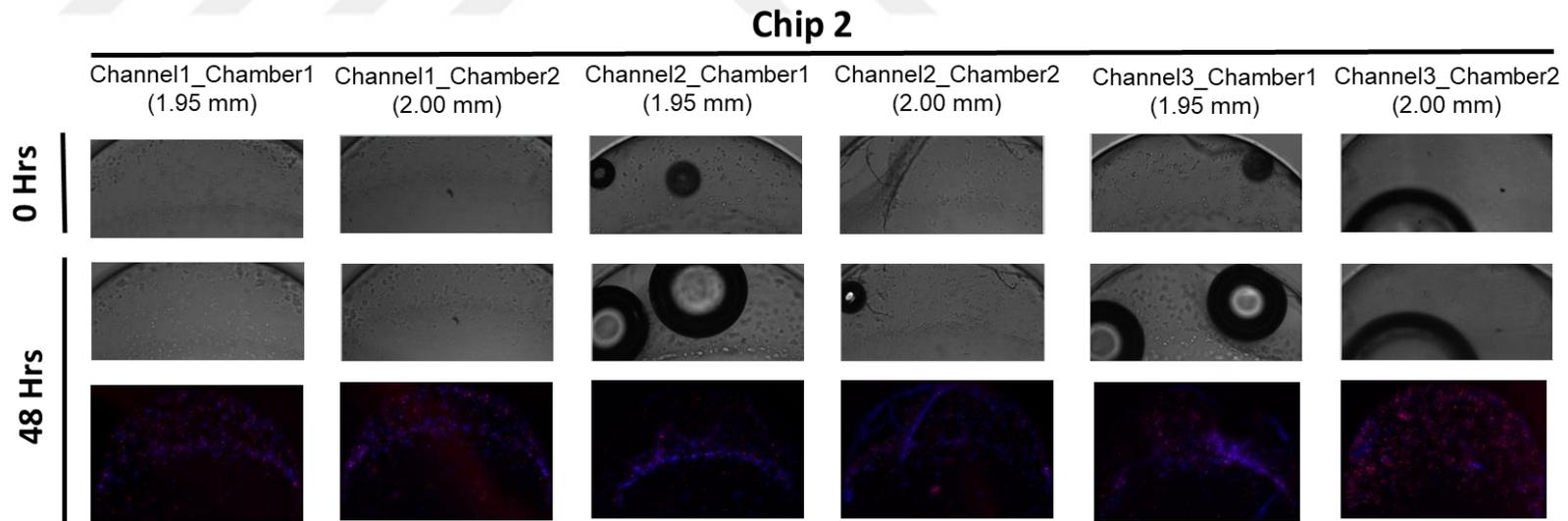|	Chip 2											
	Channel1_Chamber1 (1.95 mm)		Channel1_Chamber2 (2.00 mm)		Channel2_Chamber1 (1.95 mm)		Channel2_Chamber2 (2.00 mm)		Channel3_Chamber1 (1.95 mm)		Channel3_Chamber2 (2.00 mm)	
	4x	10x	4x	10x	4x	10x	4x	10x	4x	10x	4x	10x
Day 0 FL												
Day 0												
Day 0 BF												
Area	72800	349107	60671	241896	71468	408348	73623	310227	84504	472959	64226	424209
Day 1 FL												
Day 1												
Day 1 BF												
Area	84440	459040	70702	296757	89521	544680	88511	370932	98662	587234	66205	424209

C. Cell Growth Analysis for Targeted-RFP MCF-7 Cells in Different Chambers During 48 Hours of Experiment in Chip #2 (Continue).

	Chip 2											
	Channel1_Chamber1 (1.95 mm)		Channel1_Chamber2 (2.00 mm)		Channel2_Chamber1 (1.95 mm)		Channel2_Chamber2 (2.00 mm)		Channel3_Chamber1 (1.95 mm)		Channel3_Chamber2 (2.00 mm)	
	4x	10x	4x	10x	4x	10x	4x	10x	4x	10x	4x	10x
Day 2 FL												
Day 2												
Day 2 BF												
Area	101730		102823		110054		113778		102230		107747	

D. 10X Pictures for Cell Growth Analysis for Targeted-RFP MCF-7 Cells in Different Chambers During 48 Hours of Experiment in Chip #2.

E. Cell Growth Analysis for Targeted-RFP MCF-7 Cells in Different Chambers During 48 Hours of Experiment in Chip #3.

	Chip 3											
	Channel1_Chamber1 (1.95 mm)		Channel1_Chamber2 (2.00 mm)		Channel2_Chamber1 (1.95 mm)		Channel2_Chamber2 (2.00 mm)		Channel3_Chamber1 (1.95 mm)		Channel3_Chamber2 (2.00 mm)	
	4x	10x	4x	10x	4x	10x	4x	10x	4x	10x	4x	10x
Day 0 FL												
Day 0												
Day 0 BF												
Area	46520	157498	59497	310706	40091	181631	62221	230190	66626	260934	67056	244695
Day 1 FL												
Day 1												
Day 1 BF												
Area	53937	193161	112321	460746	26048	158848	106504	349785	85254	324434	111158	431870

78

F. **Cell Growth Analysis for Targeted-RFP MCF-7 Cells in Different Chambers During 48 Hours of Experiment in Chip #3 (Continued).**

	Chip 3											
	Channel1_Chamber1 (1.95 mm)		Channel1_Chamber2 (2.00 mm)		Channel2_Chamber1 (1.95 mm)		Channel2_Chamber2 (2.00 mm)		Channel3_Chamber1 (1.95 mm)		Channel3_Chamber2 (2.00 mm)	
	4x	10x	4x	10x	4x	10x	4x	10x	4x	10x	4x	10x
Day 2 FL												
Day 2												
Day 2 BF												
Area	45215		47441		84629		25034		75991		89519	

79

G. 10X Pictures for Cell Growth Analysis for Targeted-RFP MCF-7 Cells in Different Chambers During 48 Hours of Experiment in Chip #3.